



**HAL**  
open science

## Cutin-Derived Oligomers Act as Damage-Associated Molecular Patterns in *Arabidopsis thaliana*

Carlos J.S. Moreira, Rita Escórcio, Artur Bento, Marta Bjornson, Ana Tomé, Celso Martins, Mathieu Fanuel, Isabel Martins, Benedicte Bakan, Cyril Zipfel, et al.

► **To cite this version:**

Carlos J.S. Moreira, Rita Escórcio, Artur Bento, Marta Bjornson, Ana Tomé, et al.. Cutin-Derived Oligomers Act as Damage-Associated Molecular Patterns in *Arabidopsis thaliana*. 2024. hal-04571443

**HAL Id: hal-04571443**

**<https://hal.inrae.fr/hal-04571443>**

Preprint submitted on 23 May 2024

**HAL** is a multi-disciplinary open access archive for the deposit and dissemination of scientific research documents, whether they are published or not. The documents may come from teaching and research institutions in France or abroad, or from public or private research centers.

L'archive ouverte pluridisciplinaire **HAL**, est destinée au dépôt et à la diffusion de documents scientifiques de niveau recherche, publiés ou non, émanant des établissements d'enseignement et de recherche français ou étrangers, des laboratoires publics ou privés.



Distributed under a Creative Commons Attribution - NonCommercial - NoDerivatives 4.0 International License

1 **Cutin-Derived Oligomers Act as Damage-Associated Molecular Patterns in**  
2 ***Arabidopsis thaliana***

3  
4 Carlos J.S. Moreira<sup>a</sup>, Rita Escórcio<sup>a</sup>, Artur Bento<sup>a</sup>, Marta Bjornson<sup>b,f</sup>, Ana S.  
5 Tomé<sup>a</sup>, Celso Martins<sup>a,g</sup>, Mathieu Fanuel<sup>c,d</sup>, Isabel Martins<sup>a</sup>, Benedicte Bakan<sup>d</sup>,  
6 Cyril Zipfel<sup>b,e\*</sup> and Cristina Silva Pereira<sup>a,\*</sup>

7  
8 <sup>a</sup>Instituto de Tecnologia Química e Biológica António Xavier, Universidade Nova de Lisboa,  
9 Oeiras, Portugal.

10 <sup>b</sup>Institute of Plant and Microbial Biology, Zurich-Basel Plant Science Center, University of  
11 Zurich, Zurich, Switzerland.

12 <sup>c</sup>PROBE research infrastructure, BIBS Facility, INRAE, Nantes, France.

13 <sup>d</sup>Research Unit Biopolymers Interaction Assemblies, INRAE, Nantes, France.

14 <sup>e</sup>The Sainsbury Laboratory, University of East Anglia, Norwich Research Park, Norwich, United  
15 Kingdom.

16 <sup>f</sup>Present address: Department of Sciences, University of California, Davis, USA.

17 <sup>g</sup>Present address: Center for Integrative Genomics, Faculty of Biology and Medicine, University  
18 of Lausanne, Lausanne, Switzerland.

19

20

21 \*Corresponding authors: Cyril Zipfel ([cyril.zipfel@botinst.uzh.ch](mailto:cyril.zipfel@botinst.uzh.ch)) and Cristina  
22 Silva Pereira ([spereira@itqb.unl.pt](mailto:spereira@itqb.unl.pt))

23

24 **Abstract**

25 The cuticle constitutes the outermost defensive barrier of most land plants. It  
26 comprises a polymeric matrix – cutin, surrounded by soluble waxes. Moreover,  
27 the cuticle constitutes the first line of defense against pathogen invasion, while  
28 also protecting the plant from many abiotic stresses. Aliphatic monomers in  
29 cutin have been suggested to act as immune elicitors in plants. This study  
30 analyses the potential of tomato cutin oligomers to act as damage-associated  
31 molecular patterns (DAMPs) able to induce a rapid immune response in the  
32 model plant *Arabidopsis*. Cutin oligomeric mixtures led to Ca<sup>2+</sup> influx and MAPK  
33 activation in *Arabidopsis*. Comparable responses were measured for cutin,  
34 which was also able to induce a reactive oxygen species (ROS) burst.  
35 Furthermore, treatment of *Arabidopsis* with cutin oligomers resulted in a unique

36 transcriptional reprogramming profile, having many archetypal features of  
37 pattern-triggered immunity (PTI). Targeted spectroscopic and spectrometric  
38 analyses of the cutin oligomers suggest that the elicitors compounds consist  
39 mostly of two up to three 10,16-dihydroxyhexadecanoic acid monomers linked  
40 together through ester bonds. This study demonstrates that cutin breakdown  
41 products can act as DAMPs; a novel class of elicitors deserving further  
42 characterization.

43

#### 44 **Introduction**

45 Plants occupied land environments approximately 450 million years ago  
46 (Delwiche and Cooper, 2015). The transition from water to land habitats  
47 exposed plants to numerous challenges imposed by an extremely desiccating  
48 environment (Waters, 2003). To control water loss, protect against UV radiation  
49 and pathogens, and reinforce the epidermal cell layer, plants developed a  
50 hydrophobic barrier – the cuticle (Martin and Rose, 2014; Fich et al., 2016). The  
51 cuticle is composed of a polymeric matrix of cutin to which organic solvent  
52 soluble lipids (waxes) associate (Yeats and Rose, 2013). In addition, cutin  
53 interaction with the polysaccharides that build up the epidermal cell walls has  
54 been proposed (Philippe et al., 2020a; Xin and Fry, 2021), but the nature of  
55 such anchoring remains uncertain.

56 During infection of the aerial organs of plants, fungal spores release  
57 cutin-degrading enzymes – cutinases, having esterase activity (Longhi and  
58 Cambillau, 1999) that can disrupt the polymeric matrix and release cutin-derived  
59 molecules. Perception of these molecules by the fungus increases the  
60 production of cutinases that breach the cuticle barrier, thus allowing the fungus  
61 to invade the plant organ (Kolattukudy et al., 1995).

62 To fend off pathogen invasion, plants have developed a highly  
63 specialized mechanism to sense biotic threats by using cell surface pattern  
64 recognition receptors (PRRs)(Zipfel, 2014). These receptors perceive pathogen-  
65 associated molecular patterns (PAMPs) and damage-associated molecular  
66 patterns (DAMPs), derived from the invading pathogens or from the breakdown  
67 of plant tissues, respectively (Zipfel, 2014). Cutin aliphatic monomers (*i.e.* the  
68 major basic elements composing the cutin polymer) have been proposed as  
69 DAMPs due to their ability to induce some elements of a canonical immune

70 response, namely the production of reactive oxygen species (ROS) in  
71 cucumber, rice and *Arabidopsis thaliana* (hereafter *Arabidopsis*), and the  
72 upregulation of defense-related genes in rice and *Arabidopsis* (Kauss et al.,  
73 1999; Kim et al., 2008; Park et al., 2008). Exogenous application of monomers  
74 obtained from plants having augmented cuticular permeability (*SISHN3*-OE),  
75 increased the resistance of Micro-Tom tomato plants against the fungal  
76 pathogen *Botrytis cinerea*, and activated defense responsive genes (Buxdorf et  
77 al., 2014); however, the nature of the elicitor(s) remains unresolved. Cutin  
78 aliphatic monomers were also reported to induce the production of antimicrobial  
79 compounds (Serrano et al., 2014). Although cutin monomers have been  
80 proposed as DAMPs, their capabilities to elicit other important hallmark early  
81 immune responses, for example intracellular calcium influx and activation of  
82 mitogen-activated protein kinases (MAPKs), have never been observed  
83 (Serrano et al., 2014; Hou et al., 2019). Also, it is unclear if the tested cutin  
84 aliphatic monomers are the most potent class of cutin-derived DAMPs.  
85 Esterase-based degradation of cutin progresses through ester-cleavage, likely  
86 releasing cutin oligomers and not only monomers (Beneloujaephajri et al.,  
87 2013). This raises the hypothesis that cutin oligomers act as DAMPs, similar to  
88 that proposed for cutin monomers.

89 To investigate the hypothesis that cutin oligomers (COMs) can activate  
90 PTI responses, the cutin polymer was first isolated from tomato peel (Moreira et  
91 al., 2020; Bento et al., 2021), and subsequently broken down through a mild  
92 chemical hydrolysis to generate COMs. The ability of the produced COMs to  
93 activate calcium influx, MAPK activation and transcriptional reprogramming in  
94 *Arabidopsis* was investigated. The results clearly indicate that COMs act as  
95 DAMPs. Spectroscopy and spectrometry analyses suggested that the elicitors  
96 are dimers and/or trimers consisting mostly of esterified 10,16-  
97 dihydroxyhexadecanoic acid units (dihydroxy-C16 acid), one of which possibly  
98 methylated. The hypothesis that cutin disruption releases oligomers able to act  
99 as DAMPs is discussed in detail.

100

## 101 **Results and discussion**

102 *Cutin polymer activates a ROS burst in Arabidopsis*

103 We hypothesized that the degradation of the plant polyester cutin is coordinated  
104 with the release of polymeric/oligomeric variants capable of eliciting hallmark  
105 early plant immune responses. We first tested a cutin polymeric variant ability to  
106 induce a ROS burst in *Arabidopsis*. *Arabidopsis* is a well-established model  
107 plant for studying PTI due to the diversity of established protocols and plant  
108 resources, including characterized mutants and reporter lines (Felix et al.,  
109 1999). The ROS burst was measured through a well-established protocol that  
110 detects a luminescence signal produced in the presence of H<sub>2</sub>O<sub>2</sub> due to  
111 peroxidase (here, horseradish peroxidase, HRP)-mediated conversion of  
112 luminol (Zhu et al., 2016).

113 To obtain the cutin, an ionic liquid extractant was applied to isolate a  
114 highly pure cutin polymer (hereafter simply referred as cutin), showing minor  
115 ester cleavage (Moreira et al., 2020). This method ensures faster and simpler  
116 recovery of cutin compared to the conventional enzyme-based isolation  
117 (Moreira et al., 2020). Cutin was purified from tomato pomace since its high  
118 availability as an agroindustry residue (European Commission, 2021) enables  
119 the production of large amounts of polymeric structures. Moreover, previous  
120 studies showed that cutin purified with an ionic liquid from tomato pomace  
121 (consisting of peels, seeds and stems) is virtually similar to that obtained from  
122 the tomato peel fraction alone (Escórcio et al., 2022).

123 Exposure of seedlings of *Arabidopsis* to cutin (suspension in MilliQ water)  
124 resulted in a clear ROS burst (Fig. 1A-B and Supplemental Fig. S1). Flg22, a  
125 22-amino acid peptide derived from bacterial flagellin, is a well-established  
126 strong inducer of plant immunity (Felix et al., 1999; Correia et al., 2020) (used  
127 here as positive control). The effect was reproducible, and the response was  
128 not depleted at 45 min post-treatment (Fig. 1B). On the contrary, pure  
129 compounds (commercially available), which are representative of tomato cutin  
130 constituents: long chain fatty acids, hydroxycinnamic acids or fatty acid  
131 monoglycerides having variable side chains, did not induce a ROS burst under  
132 the tested conditions (Fig. 1C, Supplemental Fig. S2). Cutin hydrolysates, which  
133 are obtained by an extensive hydrolysis of the cutin, consist almost exclusively  
134 of aliphatic monomers with a few aromatic monomers (Escórcio et al., 2022).  
135 These hydrolysates also did not elicit a ROS burst (Fig. 1D). Collectively, the  
136 results suggest that once the polymeric backbone of the plant polyester is

137 deconstructed to its composing monomeric pieces, its capability to elicit a ROS  
138 burst is lost; hence some preservation of the polymeric backbone might be  
139 required for the eliciting of a ROS burst in *Arabidopsis*.

140 To test if small chains of monomers linked together through ester  
141 linkages; *i.e.* oligomers (<7), could act as elicitors, we prepared cutin oligomeric  
142 mixtures (COMs). To produce these, cutin was depolymerized through a mild  
143 chemical hydrolysis and the released molecules were collected (*see Materials*  
144 *and Methods*). The produced COMs were unable to trigger a ROS burst (Fig.  
145 1E). However, no effect was detected when the seedlings were co-treated with  
146 flg22 and COM, although flg22 alone clearly induced a ROS burst (Fig. 1F).  
147 This result suggests that constituents of the COM preparation interfered with the  
148 reporter of luminescence. In fact, the COM contains phenolic compounds  
149 (Supplemental, Table S1) and phenol oxidation has been reported to inactivate  
150 HRP activity in a concentration dependent mode (*i.e.* ratio enzyme:inhibitor)  
151 (Mao et al., 2013). Cutin hydrolysates (mixture of all hydrolysable cutin  
152 monomers) also contain low levels of phenolic compounds (Escórcio et al.,  
153 2022). There are alternative methods for ROS measurement; for example, DAB  
154 staining has been used to detect the accumulation of intracellular ROS in  
155 response to treatment with cutin aliphatic monomers, specifically hydroxy  
156 palmitic acid (HPA) (Kim et al., 2008; Park et al., 2008). Thus, while we  
157 observed that cutin aliphatic monomers did not induce an apoplastic ROS burst  
158 using a luminol-based assay, we cannot disregard the possibility that  
159 accumulation of intracellular ROS might occur at extended post-treatment  
160 periods.

161 The results show that treatment of *Arabidopsis* with cutin induced a ROS  
162 burst (Fig. 1A) but not any of the tested pure cutin constituents (Fig. 1C). Due to  
163 the aforementioned technical limitation, to further test COMs activity as potential  
164 elicitors of plant immunity, we converged towards the calcium response -  
165 another hallmark early immune response.

166

167 *Cutin and COMs, but not cutin hydrolysates, activate a calcium influx in*  
168 *Arabidopsis*

169 Both cutin and COMs showed a clear and reproducible induction of calcium  
170 influx in *Arabidopsis* plants expressing aequorin (Fig. 2A, 2B), a widely used

171 calcium activated reporter of immune responses in plants (Mithöfer and Mazars,  
172 2002). The response patterns were however different: cutin response was  
173 bimodal with maximum values at 3 min and 12 min (Fig. 2A), whereas COM  
174 response was monomodal with a maximum between 3 and 5 min (Fig. 2B). This  
175 result suggests that cutin may comprise several classes of chemical elicitors,  
176 one of which is prevalent in the COM fraction. *Nicotiana benthamiana* plants  
177 expressing aequorin (Segonzac et al., 2011) when exposed to COMs also  
178 showed a calcium influx having a monomodal response-type (Supplemental Fig.  
179 S3A). Since the eliciting molecules were similarly recognized by both tested  
180 plants, the elicitors are likely not species-specific.

181 Finally, no induction of a calcium influx was observed upon treatment of  
182 *Arabidopsis* seedlings with either HPA or cutin hydrolysates increasing  
183 concentrations (Supplemental Fig. S3B-C). Collectively, these data validate the  
184 opening hypothesis that cutin small oligomers may act as elicitors of PTI. Mild  
185 deconstruction of the polymer potentiates its capability to induce a calcium  
186 influx in *Arabidopsis*, but its complete depolymerization abolished this eliciting  
187 effect.

188

#### 189 *Cutin oligomers trigger MAPK activation in Arabidopsis*

190 PTI signaling events occurring downstream to elicitor perception involve the  
191 activation of MAP kinases (Yu et al., 2017; DeFalco and Zipfel, 2021).  
192 Accordingly, the capabilities of COM to activate MAP kinases in *Arabidopsis*  
193 Col-0 seedlings was evaluated. This immunoblot-based assay allows the  
194 detection of the phosphorylated (active) forms of MAPK 3, 4, 6 and 11 during  
195 PTI signaling (Willmann et al., 2014). Short (10 min) exposure of *Arabidopsis*  
196 seedlings to COM activated hallmark MAPK activation; similar to that observed  
197 when the plants were exposed to flg22 (Fig. 3). In addition to the wild type  
198 plants, three mutants were also tested, single: *cerk1-2* (Ranf et al., 2011),  
199 double: *bak1-5 bkk1* (Roux et al., 2011), and triple: *bak1-5 bkk1 cerk1 (bbc)*  
200 (Xin et al., 2016). CHITIN ELICITOR RECEPTOR KINASE 1 (CERK1) is a  
201 common co-receptor for LysM-type PRRs (Macho and Zipfel, 2014) while  
202 BRASSINOSTEROID INSENSITIVE 1-ASSOCIATED KINASE 1 (BAK1) and  
203 BAK1-LIKE KINASE 1 (BKK1) are common co-receptors for leucine-rich repeat-  
204 type PRRs (Tang et al., 2017). Thus, differences in the response pattern of the

205 selected mutants may reveal potential families of PRR(s) that recognize the  
206 elicitor(s) within COM. The results showed that COM induced a clear activation  
207 of MAP kinases in all the mutants tested, similar to that observed in the wild-  
208 type plants (Fig. 3). The observation that MAPK activation was similar in all  
209 mutants is suggestive of a perception mechanism independent on the families  
210 of PRRs known to associate with CERK1 and SERKs. Ultimately, these results  
211 suggest that COMs triggered a MAPK-mediated signaling cascade, opening the  
212 hypothesis that COM exposure also involves transcriptional reprogramming.

213

214 *Cutin oligomers treatment induced a transcriptional reprogramming consistent*  
215 *with activation of PTI*

216 We evaluated the transcriptional reprogramming in *Arabidopsis* seedlings upon  
217 a 30-min treatment with COM compared to mock control (RNA-seq). Previous  
218 studies covering distinct PTI elicitors showed significant responses at 30 min  
219 post-treatment (Bjornson et al., 2021). Principal components analysis (PCA)  
220 demonstrates that their transcriptomic profiles are clearly separating from each  
221 other (Supplemental Fig. S4). A total of 528 differentially expressed genes  
222 (DEGs) resulted from the COM treatment, of which 479 genes were  
223 upregulated, while only 49 were downregulated compared to the mock  
224 treatment (Fig. 4A). Enriched gene ontology (GO) categories were only  
225 obtained for the subset of upregulated genes due to the small number of  
226 downregulated genes. An enrichment for terms related to activation of plant  
227 immunity, particularly ‘response to wounding’ and ‘response to other organism’  
228 was noticed (Fig. 4B).

229 The observed transcriptional reprogramming induced by the COM  
230 treatment was compared to that induced (*i.e.* upregulated) by seven other well-  
231 characterized elicitors of plant immunity, recently reported by Bjornson *et al.*  
232 (Bjornson et al., 2021). The COM effect presents similarity with that of the other  
233 elicitors: 140 induced genes (~30%) responded to COM and the other PTI  
234 elicitors (Fig. 4C). The transcriptional reprogramming induced by COM has  
235 however some uniqueness since 105 induced genes (~20%) were not induced  
236 by any of the other tested elicitors (Fig. 4C). In fact, such level of specificity in  
237 transcriptional reprogramming was previously only observed for flg22 (Bjornson  
238 et al., 2021) (Fig. 4C). The lower number of induced genes by COM treatment



239 could be related to the single time point used, differently from the other elicitors  
240 of PTI where multiple timepoints were used. The genes induced only by COM  
241 (and not by the other elicitors) were compared with genes found to be  
242 upregulated under abiotic stress (seven types of stresses were considered, see  
243 *Materials and Methods*). We observed that among these, 32 genes were  
244 induced solely by COM and not by any of the abiotic stresses (Supplemental  
245 Table S2 and Table S3); further suggestive of a certain degree of uniqueness  
246 on the COM's effect.

247 The uniqueness of the COM treatment was further demonstrated through  
248 a correlation analysis of all elicitor transcriptomic datasets at the 30-min  
249 timepoint (Fig. 4D). At this timepoint, COM effect is not well correlated with any  
250 of the other tested elicitors; for example, bacterial hydroxy-fatty acid (3-OH-FA)  
251 and fungal chitooctamer (CO8). It also showed no correlation with the effect of  
252 oligogalacturonides (OGs) originating from plant cell wall pectin degradation.  
253 Cutin anchoring to the cell wall is a long-standing debate, but the involvement of  
254 polysaccharide-based moieties has been suggested (Philippe et al., 2020b).  
255 Polysaccharides can be found at very low amounts in cutin isolated using the  
256 ionic liquid extractant (Bento et al., 2021), but it remains an unresolved question  
257 if the detected polysaccharide-moieties are covalently linked to cutin. No  
258 glycoside-type linkages were detected in the NMR spectral fingerprint of a  
259 highly concentrated COM sample: 40 mg to allow the detection of low-intensity  
260 signals (Supplemental Fig. S5A). Several molecules derived from cell wall  
261 polysaccharides can act as elicitors, for example OGs (Ferrari et al., 2013),  
262 cellobiose (de Azevedo Souza et al., 2017), arabinoxylan oligosaccharides  
263 (Mélida et al., 2020) and mixed-linked  $\beta$ -1,3/1,4-glucans (Rebaque et al., 2021).  
264 However, the reported amounts for their eliciting effects (de Azevedo Souza et  
265 al., 2017) usually range from  $\mu\text{g}\cdot\text{mL}^{-1}$  to  $\text{mg}\cdot\text{mL}^{-1}$ . These levels are higher than  
266 those detected in the COM preparations that were observed to contain only  
267 picograms of hydrolysable sugars *per* mg of COM (Supplemental Fig. S5B).  
268 The acquired data thus indicate that the molecules within the COM preparation  
269 acting as elicitors have a lipidic nature.

270

271 *Guiding principles on the chemistry of COMs that are able to elicit a rapid*  
272 *immune response in Arabidopsis*

273 COM preparations have been shown to consist of oligomers and monomers  
274 (Escórcio et al., 2022). During infection, pathogens can secrete enzymes able  
275 to hydrolyze ester-type linkages present in cutin (Serrano et al., 2014); breaking  
276 the structural integrity of the cutin barrier to allow pathogen invasion of the  
277 infected plant tissue. To mimic such progressive attack of cutin, after obtaining  
278 a COM preparation, the non-hydrolyzed cutin fraction was recovered. The  
279 recovered cutin was subjected to a second round of mild hydrolysis and  
280 subsequently processed to obtain a COM II fraction. In *Arabidopsis* plants, the  
281 signal-intensity of the COM II induced calcium influx was >2-fold higher than  
282 that observed after COM treatment (Supplemental Fig. S6). This observation  
283 suggests that COM II might be more enriched in active elicitors compared to  
284 COM.

285 The free monomers were detected (and quantified) by GC-MS analysis,  
286 which also differentiates the methylated derivatives formed during the cleavage  
287 of esters through the methanolysis reaction (Supplemental, Table S1). The  
288 presence of oligomers was directly inferred from the detection of both primary  
289 (PAE) and secondary aliphatic esters (SAE) through NMR analyses, specifically  
290 in the HSQC spectral fingerprints of either COM preparation (Fig. 5A). The  
291 integration of their corresponding <sup>1</sup>H NMR signals, relative to an internal  
292 standard, was used to infer the relative amount of PAE (*i.e.* linear) and SAE (*i.e.*  
293 branched) (Fig. 5B). Both types of esterification have been reported before in  
294 the spectral fingerprint of several cutin variants (Moreira et al., 2020; Bento et  
295 al., 2021; Escórcio et al., 2022). The estimated relative abundances of methyl  
296 esters in COM range from 40 to 70% of the total esters, consistent with the GC-  
297 MS data (Supplemental, Table S1). To depolymerize all present oligomers, the  
298 COM was subjected to hydrolysis and reanalyzed by GC-MS. Comparison of  
299 the resultant monomeric profiles of the COM and the resulting hydrolysate,  
300 exposed monomers increasing in abundance after hydrolysis (Supplemental,  
301 Table S1). The major aliphatic monomer of cutin, dihydroxy-C16 acid, is likely  
302 the major building block of the oligomers, distantly followed by 9,10-epoxy-18-  
303 hydroxyoctadecanoic acid, nonanedioic acid and hexadecanedioic acid.

304 A preliminary LC-MS/MS analysis was performed targeting the exact  
305 masses of dihydroxy-C16 acid dimers and trimers, carrying or not one  
306 methylation (Supplemental, Table S4A). Pure HPA was used to setup the

307 method (see *Materials and Methods*). The given outputs (Compound Discovery  
308 3.2) were unsupervised since the software automatically computes the most  
309 likely ions/adducts to be generated in negative/positive modes for each given  
310 mass (Supplemental, Table S4B). In both COMs, dimers were putatively  
311 identified, namely two dihydroxy-C16 acid molecules esterified, methylated or  
312 not – DP2 (Fig. 6A-B, Supplemental Fig. S7A-B). A trimer of dihydroxy-C16 acid  
313 molecules, carrying or not one methylation, was putatively identified only in  
314 COM II – DP3 (Fig. 6C-D, Supplemental Fig. S7C-D). These molecules can be  
315 a linear chain, yet one side-branch is possible (Fig. 6E-F). The NMR  
316 quantification data suggest that linear esters are in average two- to three-fold  
317 more abundant than branched esters (Fig. 5B), accordingly the linear DP3 chain  
318 is more likely to exist.

319 A MALDI-TOF method was developed to screen for the putative  
320 presence of oligomers up to octamers species (Supplemental Fig. S8). The  
321 MALDI-TOF analyses showed the presence of the most abundant free  
322 monomers in COM and COM II, some of which in the methylated form  
323 (Supplemental, Table S5). The controls - cutin and COMs hydrolysates - also  
324 contain the same non-methylated monomers (Supplemental, Table S5). In the  
325 COMs, dimers were identified, namely DP2, methylated or not (Fig. 7A),  
326 consistent with the LC-MS/MS. To selectively observe species capable of self-  
327 ionization such as aromatics, samples analyzed by MALDI-TOF were also  
328 analyzed without addition of ionization matrix (LDI-TOF). On the LDI-TOF  
329 spectra, other dimers detected consist of a dihydroxy-C16 acid esterified to  
330 coumaric acid without, or with one or two methylations - DP2c (Supplemental  
331 Fig. S9). The DP2c methylated molecules were only detected in the COM. The  
332 cutin hydrolysate (control) showed the presence of the non-methylated forms of  
333 DP2 in MALDI-TOF and DP2c in LDI-TOF (Supplemental, Table S5). NMR  
334 analyses of 40 mg of either COM, showed the presence of esterified aromatics  
335 only in COM (Supplemental, Fig. S10). Finally, the methylated-DP3 and, its  
336 non-methylated form, were identified in COM II (Fig. 7B), regardless of  
337 undetected in COM possibly due to lower relative abundance. Collectively the  
338 data on the COMs (and cutin hydrolysates) suggest that amongst the identified  
339 oligomeric species, the best PTI elicitor candidates are linear dimers or trimers  
340 composed of dihydroxy-C16 acid units, one of which possibly methylated.

341

## 342 **Conclusions**

343 The plant cell wall barrier is an important interface during plant–microbe  
344 interactions, where cutin is the outermost polymeric component. Plants are able  
345 to recognize damages caused by pathogens, and elicit immune responses for  
346 example upon recognition of cell wall-derived fragments acting as DAMPs. As  
347 such, the cell wall barrier orchestrates key responses of the plant interaction  
348 with the surrounding environment. This rationale has defined the major  
349 hypothesis of our study, namely that cutin oligomers act as DAMPs able to  
350 trigger plant immune responses. In *Arabidopsis*, cutin oligomers (COMs),  
351 obtained through methanolysis of tomato pomace cutin, elicited several  
352 hallmark immune responses, including calcium influx (Fig. 2) and MAPK  
353 activation (Fig. 3), and a transcriptional response comprising features similar to  
354 those activated by well-characterized elicitors (Fig. 4). The perception  
355 mechanism of the COMs, which was observed to be independent of  
356 BAK1/BKK1 and CERK1 co-receptors, remains yet unresolved.

357 Chemical analyses identified that the COMs contain trimers and dimers  
358 (Fig. 6-7). The strongest elicitor candidates are the dihydroxy-C16 acid dimers  
359 (DP2) or trimers (DP3) carrying a methylation. DP2, methylated or not, were  
360 detected in both COMs. On the contrary, the DP3 and DP2c (dihydroxy-C16  
361 acid esterified to coumaric acid), carrying or not methylation, were only detected  
362 in COM II and COM, respectively. The non-methylated DP2 and DP2c were  
363 present in cutin hydrolysates unable to elicit a calcium burst, though the  
364 threshold for PTI activation remains unknown. The methylation increases the  
365 oligomer's lipophilicity, possibly favoring its diffusion; a hypothesis that requires  
366 focused analysis. Methyl-esters are, for example, present in seeds (Annarao et  
367 al., 2008) and vegetable oil (di Pietro et al., 2020). However, the isolated cutin  
368 polymer, which is deprived of methyl-esters, elicited a rapid ROS burst (Fig. 1A-  
369 B) and calcium influx (Fig. 2A). This observation questions the requirement of  
370 methylation for immune activation. Fungal lipases can generate methyl esters,  
371 for example from vegetable oil (Li et al., 2007). In plants, the modification of  
372 cutin degradation products by microbial methyl-transferases remains unknown  
373 in the context of PTI. However, methylation to potentiate the eliciting effect of

374 cutin oligomers, may inspire alternative biotechnological valorization paths for  
375 fruit pomaces.

376 Both the cutin polymer (with minor degree of structural damage) and the  
377 generated oligomers acted as PTI elicitors. Previous work by others showed  
378 that some cutin monomers also activated some aspects of plant immunity  
379 (Kauss et al., 1999; Kim et al., 2008; Park et al., 2008). A step-by-step  
380 activation of specific elements of plant immunity by cutin having distinct degrees  
381 of structural damage, constitutes an appealing concept that deserves further  
382 investigation. The release of oligomeric elicitors during plant infection requires  
383 validation to attain a mechanistic understanding of cutin's multiple functions in  
384 plant-pathogen interactions. The identity of the precise COM elicitors remain  
385 putative, and efficient syntheses are needed to obtain pure compounds.  
386 However, COMs clearly constitute a new class of DAMPs. Hence, their  
387 production from agro-industrial residues constitutes a promising value chain and  
388 may support development of sustainable agricultural bio-based treatments to  
389 increase disease resistance.

390

## 391 **Materials and Methods**

392

393 **Plant Growth Conditions** *Arabidopsis thaliana* Col-0 seeds were germinated  
394 on soil and plants were grown for four-weeks in an Aralab Fitoclima climate  
395 chamber with  $150 \mu\text{mol}\cdot\text{s}^{-1}\cdot\text{m}^{-2}$  light intensity, following a 10 h/14 h day/night  
396 cycle, under constant temperature of 20 °C and 60 % humidity. Plants were  
397 watered automatically for 10 min three times *per week*. *Arabidopsis thaliana*  
398 Col-0 and the mutants *bak1-5 bkk1*, *cerk1-2<sup>AEQ</sup>* and *bbc* (Ranf et al., 2011;  
399 Roux et al., 2011; Xin et al., 2016), all in the Col-0 background, seeds were  
400 germinated on plates with 0.5 x Murashige and Skoog (MS) basal salt mixture  
401 supplemented with 1 % (w/v) sucrose and 0.9 % (w/v) phytoagar. After four  
402 days, seedlings were transferred to 24-well sterile culture plates containing 0.5x  
403 MS mixture supplemented with 1 % (w/v) sucrose and grown in sterile  
404 conditions in a Aralab Fitoclima climate chamber with  $120 \mu\text{mol}\cdot\text{s}^{-1}\cdot\text{m}^{-2}$  light  
405 intensity, following a 16 h/8 h day/night cycle, under temperatures of 20 °C  
406 during the day and 18 °C at night. The growth period was 8-days, 11-days or  
407 14-days depending of the subsequent assays.

408 *Solanum lycopersicum* 'Moneymaker' seeds were germinated on soil and  
409 plants were grown for four weeks on a Conviron climate chamber with  
410  $120 \mu\text{mol}\cdot\text{s}^{-1}\cdot\text{m}^{-2}$  light intensity, following a 12 h/12 h day/night cycle, under  
411 temperatures of 21 °C during the day and 19 °C at night and constant humidity  
412 of 60 %. Plants were watered manually three times *per week*.

413 *Nicotiana benthamiana* plants seeds were germinated on soil and plants grown  
414 for four weeks on a greenhouse room with  $150 \mu\text{mol}\cdot\text{s}^{-1}\cdot\text{m}^{-2}$  light intensity,  
415 following 16 h/8 h day/night cycle, under constant temperature of 24 °C. These  
416 plants were watered automatically daily for 20 min.

417

418 **Cutin Extraction.** Cutin was extracted from tomato pomace as previously  
419 described (Moreira et al., 2020). The tomato pomace was obtained from Sumol  
420 + Compal, SA., and dried at 60 °C for one week until constant weight. Dry  
421 pomace was then milled using a Retsch ZM200 electric grinder (granulometry  
422 0.5 mm; 10000 rpm) and stored at room temperature until further use. In brief,  
423 tomato pomace and cholinium hexanoate were mixed (1:10) and incubated for 2  
424 h at 100 °C. The reaction was stopped by the addition of 80 mL of DMSO *per*  
425 gram of tomato pomace. The polyester was recovered by filtration using a nylon  
426 membrane filter (0.45  $\mu\text{m}$ ). Purification was obtained by washing with an excess  
427 of deionized water to remove all traces of DMSO. Purified cutin were then  
428 freeze dried and stored at room temperature for further use. Suspensions of the  
429 purified cutin powder were prepared in MiliQ water for testing purposes.

430

431 **Cutin Hydrolysis.** To obtain a cutin oligomeric mixture (COM), a sodium  
432 methoxide-catalyzed methanolysis was performed by mixing 0.5 g of cutin with  
433 20 mL of a solution of sodium methoxide (0.1M) in anhydrous methanol, at 40 °C  
434 for 2 h without stirring. At the end of the reaction, the mixture was cooled to  
435 room temperature and centrifuged (4 °C, 30 min, 4000 g) to recover the non-  
436 hydrolyzed cutin fraction. The supernatant (hydrolyzed fraction) was acidified to  
437 pH 3–3.5 by addition of HCl 37 % and subsequently centrifuged (4 °C, 30 min,  
438 4000 g). The resulting precipitate was recovered, and the supernatant extracted  
439 three times by dichloromethane/water partition to release the hydrolysates; and  
440 sodium sulphate anhydrous was added to remove traces of water. The solution  
441 was concentrated under a constant nitrogen flux at 40 °C. To obtain cutin or

442 COM hydrolysates, a sodium hydroxide alkaline hydrolysis was performed by  
443 mixing a solution of 0.5 M NaOH in methanol/water (1:1, v/v) at 95 °C with the  
444 cutin/COM powder, for 4 h. At the end of the reaction, the mixture was cooled to  
445 room temperature, then acidified to pH 3/3.5 with 1 M HCl, and subsequently  
446 extracted by dichloromethane/water partition to release the hydrolysable  
447 constituents. The solution was concentrated under a constant nitrogen flux at 40  
448 °C.

449

450 **Immune assays.** Leaf discs (collected using a 4-mm biopsy punch) or  
451 seedlings were transferred to white 96-well plates (one leaf disc or seedling *per*  
452 well) and equilibrated overnight in sterile ultrapure water (ROS measurements)  
453 or coelenterazine solution (Calcium measurements). The following day, the  
454 equilibration solution was removed, and replaced with a solution containing 100  
455  $\mu\text{g}\cdot\text{mL}^{-1}$  up to 2  $\text{mg}\cdot\text{mL}^{-1}$  of COM, cutin hydrolysate, hydroxy palmitic acid (HPA)  
456 or cutin (Calcium measurements), and mixed with 1 mM luminol, and 10  $\mu\text{g}\cdot\text{mL}^{-1}$   
457 HRP in the case of ROS measurements. Positive controls were also prepared  
458 with 100 nM (flg22 and Pep1) in MiliQ water, as well as blanks with 0.5 % (v/v)  
459 DMSO in MiliQ water or MiliQ water. Luminescence was detected and  
460 measured for 30 - 45 min using a Photech system equipped with a photon  
461 counting camera (leaf discs) or a Tecan Spark microplate reader (seedlings).

462

463 *MAPK activation* – For MAPK activation assays 14-day-old seedlings were  
464 used. The growth media was removed by inverting the plate on clean paper  
465 towels. Seedlings were treated for 10 min with 1 mL of 3  $\text{mg}\cdot\text{mL}^{-1}$  of COM, 100  
466 nM flg22 (positive control) or the corresponding mock solutions (solvent  
467 control). Two seedlings *per* treatment were dried on clean paper towels,  
468 subsequently transferred to 1.5-mL tubes and instantly frozen in liquid nitrogen.  
469 All treated seedlings were stored at -80 °C until further use. Frozen seedlings  
470 were pulverized using a nitrogen-cooled plastic micro pestle, then mixed with  
471 150  $\mu\text{L}$  of extraction buffer containing 50 mM Tris-HCl pH 7.5, 150 mM NaCl,  
472 2 mM EDTA, 10 % (v/v) glycerol, 2 mM DTT, 1 % (v/v) Igepal, and supplemented  
473 with protease and phosphatase inhibitors (equivalent to Sigma-Aldrich plant  
474 protease inhibitor cocktail and phosphatase inhibitor cocktails #2 and #3) was  
475 added. The tissue was then ground at 1800 rpm using an automatic stirrer

476 fitted with a plastic micro pestle. The tubes were centrifuged at 15,000 g for 20  
477 min at 4 °C in a refrigerated microcentrifuge. After centrifugation, 50 µL of  
478 extract were transferred to a fresh 1.5-mL Eppendorf tube. Samples were  
479 prepared for SDS-PAGE by heating at 80 °C for 10 min in the presence of 6x  
480 SDS loading buffer and 100 mM DTT.

481 Proteins were loaded to a 12 % (v/v) polyacrylamide gels, separated at  
482 120 V for  $\cong$  120 min and subsequently transferred to a PVDF membrane at 100  
483 V for 90 min at 4 °C. Membranes were then blocked for 2 h at room temperature  
484 or overnight at 4 °C in 5 % (w/v) milk in Tris buffered saline  
485 (50 mM Tris-HCl pH 7.4, 150 mM NaCl; TBS) containing 0.1 % (v/v)  
486 Tween-20 (TBS-T). Blots were probed in a 1:4000 dilution of the  
487 NEB anti-p42/p44-erk primary antibody in 5 % BSA in TBS-T for 2 h, followed  
488 by washing 4 times for 10 min each in TBS-T. Blots were then probed with a  
489 1:10000 dilution of anti-rabbit secondary antibody in 5 % milk in TBS-T for  
490 1 h, followed by washing 3 times for 5 min each in TBS-T. Finally, blots were  
491 washed for 5 min in TBS and treated with either standard ECL substrate or  
492 SuperSignal West Femto high sensitivity substrate (ThermoFisher Scientific).  
493 Blots were imaged using a Bio-Rad ChemiDoc Imaging System (Bio-Rad  
494 Laboratories).

495

496 **RNA Extraction and Sequencing.** For RNA-seq experiments, 14-day-old  
497 seedlings were grown as described above. After nine days of growth in liquid  
498 MS medium supplemented with 1 % sucrose, the medium was removed from  
499 the wells and replaced with 600 µL of fresh liquid MS per well. The following  
500 day, 400 µL of 3 mg/mL of COM in 0.5 % DMSO in MiliQ water or the  
501 corresponding mock solution were added to each well. Seedlings were treated  
502 for 30 min and then two were collected and instantly frozen in liquid nitrogen. In  
503 total, four biological replicates were generated for each treatment (COM and  
504 mock) and stored at -80 °C for further processing.

505 Frozen seedlings were pulverized while frozen using a  
506 Spex SamplePrep Geno Grinder 2010 at 1500 rpm for 90 s. Total RNA was  
507 extracted at 4 °C from two ground seedlings as previously described (Shi and  
508 Bressan, 2006) by addition of 900 µL of TRI reagent (Ambion) and 200 µL of  
509 chloroform, recovery of 400 µL from the aqueous phase, precipitation with 500



510  $\mu$ L of isopropanol and washing with 70 % ethanol. All samples were then  
511 solubilized in 30  $\mu$ L of RNase-free water. Samples were subsequently subjected  
512 to DNase treatment using a TURBO DNA-free Kit (Ambion) according to  
513 manufacturer's instructions. The reaction mix was incubated at 37 °C for 30  
514 min, after which the inactivation reagent was added and incubated for 5 min at  
515 room temperature. After centrifugation the supernatant was transferred to a new  
516 tube. Quantification and quality assessment of all RNA samples were evaluated  
517 on a TapeStation (Agilent) and RNA sequencing performed by the Beijing  
518 Genomics Institute (BGI).

519

520 **RNA-seq data processing.** For paired-end RNA sequencing (RNA-seq),  
521 libraries were generated at BGI according to the DNBSEQ stranded mRNA  
522 library system. Eight samples were indexed and sequenced using the  
523 DNBseq™ sequencing platform (20 million reads per sample). Generated  
524 FastQ files were analyzed with FastQC, and any low-quality reads were  
525 trimmed with Trimmomatic (Bolger et al., 2014).

526 All libraries were aligned to the *A. thaliana* genome assembly TAIR10  
527 with gene annotations from Ensembl Plants v.49 using the HISAT2 v.2.1.0  
528 pipeline(Kim et al., 2015) followed by read counts with HTSeq v. 0.13.5(Anders  
529 et al., 2015). All RNA-seq experiments were carried out with four biological  
530 replicates. Differential expression analysis, and quality control principal-  
531 component analysis (PCA) and MA plots were generated using the DESeq2  
532 v.1.30.0 R package(Love et al., 2014). The genes that showed  $|\log_2| > 1$ -fold  
533 changes in expression with an adjusted  
534 P value below 0.05 are defined as significantly differentially expressed genes  
535 (DEGs) in this analysis. Transcript abundance was defined as transcripts per  
536 kilobase million (TPM). Gene Ontology enrichment of the differentially  
537 expressed genes was performed with the topGO v.2.42.0 R package, using the  
538 Fisher exact test to attain significantly enriched categories.

539

540 **Comparative analysis of transcriptome modification upon elicitor**  
541 **treatment.** Differentially expressed gene lists in response to seven elicitors (3-  
542 OH-FA, CO8, elf18, flg22, nlp20, OGs, Pep1) upon treatment under similar  
543 conditions as COM were obtained from Bjornson, *et al.* (2021) (Bjornson et al.,

544 2021). This study followed a time course from 5 min to 3 h post-elicitation: a  
545 gene list was obtained for each elicitor with genes significantly induced at any  
546 time. Abiotic stress treatment analysis for seven abiotic stresses (heat, cold,  
547 drought, salt, high osmolarity, UV-B light, wounding) was also obtained from  
548 Bjornson, *et al.* (2021), based on ATH1 microarray experiments presented in  
549 Killian, *et al.* 2007 (Killian et al., 2007). This study followed a time course from 5  
550 min to 12 h post-elicitation: a gene list was obtained for each elicitor with genes  
551 significantly induced at any time up to 3 h. Comparisons and visualizations  
552 among differentially expressed genes were performed in R using the tools of the  
553 tidyverse v.1.3.1 package (Wickham et al., 2019). Spearman correlation among  
554  $\log_2$  (fold changes) for treatments was calculated using the Hmisc package in  
555 R v.4.5-0) and visualized using the corrplot package v.0.89. Annotation data for  
556 genes induced specifically by COM was obtained from the *Arabidopsis*  
557 information resource (TAIR) via Bioconductor package org.At.tair.db v.3.10.0.  
558 The raw data and the processed file are deposited in the ArrayExpress  
559 ([www.ebi.ac.uk/fg/annotate/edit/16708/](http://www.ebi.ac.uk/fg/annotate/edit/16708/)), publicly available after curation.

560

561 **Quantitative analyses of total carbohydrate content.** To evaluate the  
562 polysaccharide content, each COM sample was subjected to an acid hydrolysis  
563 (1 M H<sub>2</sub>SO<sub>4</sub> in methanol) for 4h at 90 °C. The hydrolysable sugars were  
564 recovered in the supernatant through centrifugation (18514 g, 4 °C, 20 minutes)  
565 and the pH was neutralized using 5 M NaOH in water. All samples were dried  
566 under a flux of nitrogen at room temperature. Quantification of carbohydrates in  
567 the dried hydrolysates was performed using the total carbohydrate assay kit  
568 from Sigma-Aldrich according to the manufacturer's instructions. The samples  
569 were analyzed in triplicates.

570

571 **NMR characterization of cutin oligomeric mixtures.** NMR spectra of COMs  
572 were recorded using an Avance III 800 CRYO (Bruker Biospin, Rheinstetten,  
573 Germany). All NMR spectra (<sup>1</sup>H, <sup>1</sup>H-<sup>1</sup>H COSY, <sup>1</sup>H-<sup>13</sup>C HSQC, <sup>1</sup>H-<sup>13</sup>C HMBC)  
574 were acquired in DMSO-*d*<sub>6</sub> using 5 mm-diameter NMR tubes, at 60 °C as  
575 follows: 15 mg of COMs in 400 μL of DMSO-*d*<sub>6</sub> (in triplicate) or for validation 40  
576 mg of COMs in 400 μL of DMSO-*d*<sub>6</sub>. For quantification purposes, 1.25 mg of  
577 benzene (internal standard) was added to each sample. MestReNova, Version

578 11.04-18998 (Mestrelab Research, S.L.) was used to process the raw data  
579 acquired in the Bruker spectrometers.

580

581 **GC-MS characterization of cutin oligomeric mixtures.** To release the  
582 hydrolysable constituents, the COMs were treated with a solution of 0.5 M  
583 NaOH in methanol:water (1:1 [v/v]) at 95 °C for 4 h. The mixture was cooled to  
584 room temperature and acidified to pH 3–3.5 with HCl 1 M, spiked with a known  
585 concentration of hexadecane (internal standard), and extracted three times with  
586 dichloromethane. Sodium sulphate anhydrous was added to the organic phase  
587 to remove water and concentrated under a nitrogen flow. The non-hydrolysable  
588 fraction was recovered by filtration (cellulose nitrate filter) and subsequently  
589 washed, dried, and weighted (recalcitrance). The COMs samples were also  
590 analyzed directly, *i.e.* not subjected to alkaline hydrolysis. The dried samples  
591 were derivatized in N,O-bis(trimethylsilyl)trifluoroacetamide containing 1 % (v/v)  
592 of trimethylchlorosilane in pyridine (5:1), for 30 min at  
593 90 °C. The derivatives were then analyzed by GC-MS (Agilent: 7820A GC and  
594 5977B quadrupole MS; HP-5MS column) as follows: ramp temperature 80 °C,  
595 then 2 °C·min<sup>-1</sup> to 310 °C for 15 min. The MS scan mode, with source at  
596 230 °C and electron impact ionization (EI<sup>+</sup>, 70 eV) was used for all samples.  
597 Data acquisition was accomplished by MSD ChemStation (Agilent  
598 Technologies); compounds were identified based on the equipment spectral  
599 library (Wiley-National Institute of Standards and Technology) and quantified  
600 using external standards of the major classes of the aliphatic monomers  
601 (heptadecanoic acid, hexadecanedioic acid and pentadecanol). All samples  
602 were analyzed in triplicates, each with technical duplicates.

603

604 **LC-MS/MS characterization of COMs.** The LC-MS/MS protocol was adapted  
605 from Bhunia R. *et al.* (2018) (Bhunia et al., 2018). The experiments were  
606 performed in a Q Exactive Focus™ Hybrid Quadrupole-Orbitrap™ Mass  
607 Spectrometer coupled to a Dionex Ultimate 3000 UHPLC. HPA was used as a  
608 standard and prepared in isopropanol:methanol:acetonitrile (1:1:1) at a  
609 concentration of 200 ng/μL. The samples were prepared in the same way at 1  
610 μg/μL. Separation was achieved in a Waters XBridge column C18 (2.1x150  
611 mm, 3.5 μm particle size, P/N 186003023), using a gradient of increasing

612 percentage of 20 mM ammonium formate in isopropanol (IPA): acetonitrile  
613 (ACN) (75:25) (B) and decreasing percentage of ACN:water (60:40) with 20 mM  
614 ammonium formate (A). The total method time was 77 min, the flow rate was  
615  $0.4 \text{ mL} \cdot \text{min}^{-1}$ , and the column was kept at  $37 \text{ }^\circ\text{C}$ . The data was acquired using  
616 the Xcalibur software v.4.0.27.19 (Thermo Scientific). The method consisted of  
617 several cycles of Full MS scans ( $R=70000$ ; Scan range=100-1500 m/z) followed  
618 by 3 ddMS2 scans ( $R=17500$ ; NCE 30 V) in positive and negative mode.  
619 External calibration was performed using LTQ ESI Positive/Negative Ion  
620 Calibration Solution (Thermo Scientific). Generated mass spectra were  
621 processed using Compound Discoverer 3.2 (Thermo) for small molecule  
622 identification. The search was performed against the mass list with provided  
623 molecular formulas (dimers, trimers), as well as mzCloud MS2 database, KEGG  
624 and ChEBI MS1 databases. A 3-ppm mass tolerance was used. The minimum  
625 peak intensity (MS1) for detection was  $10^6$ . A manual validation of the  
626 assignments for the identified oligomers was performed by inspection the MS2  
627 fragmentation profiles against the theoretical fragmentation generated on Mass  
628 Frontier 8.0 (Thermo). Theoretical chemical structures for the identified  
629 oligomers were generated ChemDraw 21.0.0.

630

631 **LDI-TOF and MALDI-TOF analyses of COMs and corresponding**  
632 **hydrolysates.** The samples were analyzed by laser desorption/ionization (LDI)-  
633 time-of-flight (TOF) MS and by matrix-assisted laser desorption/ionization  
634 (MALDI)-time-of-flight (TOF) MS. As control for monomers, total alkaline  
635 hydrolysate of cutin was used. As oligomers control, a batch of oligomers (DP1  
636 to DP8) were produced (Supplemental Fig. S8) from purified cutin monomers as  
637 previously described (Marc et al., 2021) with small modification. The  
638 polymerization time was reduced to 8 h and the oligomers were extracted from  
639 the polymer by hot ( $70 \text{ }^\circ\text{C}$ ) ethanol extraction.

640 For the LDI-TOF analyses, the samples were deposited on a polished  
641 steel MALDI target plate and analyzed without any preparation. For the MALDI-  
642 TOF analyses, samples were mixed with the matrix solution composed of DHB  
643 (2,5-dihydroxybenzoic acid)  $3 \text{ mg} \cdot \text{mL}^{-1}$  in 75% methanol, with 2.5 mM LiCl, in a  
644 1:3 ratio (v/v). The mixture ( $1 \text{ } \mu\text{L}$ ) was deposited on a polished steel MALDI  
645 target plate. Measurements were performed on a rapifleX MALDI-TOF

646 spectrometer (Bruker Daltonics, Bremen, Germany) equipped with a  
647 Smartbeam 3D laser (355 nm, 10000 Hz) and controlled using the Flex Control  
648 4.0 software package. The mass spectrometer was operated in reflectron mode  
649 with positive polarity for MALDI-TOF analyses and in negative polarity for LDI-  
650 TOF analyses. Spectra were acquired in the range of 180-5000 m/z. Neither  
651 the MALDI-TOF nor the LDI-TOF used in these experiments can observe the  
652 signal of the free *p*-coumaric acid.

653

654

655

656

657 **Acknowledgements**

658 The authors are thankful to Pedro Lamosa (ITQB NOVA) for support with the  
659 NMR analyses. Mass spectrometry data were generated by the Mass  
660 Spectrometry Unit (UniMS), ITQB/iBET, Oeiras, Portugal. We thank Stefanie  
661 Ranf for the gift of *cerk1-2<sup>AEQ</sup>* seeds. All members of the Silva Pereira and Zipfel  
662 labs are also thanked for useful discussions.

663

664 **Funding**

665 We acknowledge funding from the European Research Council through grant  
666 ERC 2014-CoG-647928 and from Fundação para a Ciência e Tecnologia (FCT)  
667 by Project MOSTMICRO ITQB (UIDB/04612/2020 and UIDP/04612/2020) and  
668 to the PESSOA program (Prpc n° 441.00) to Cristina Silva Pereira, and from the  
669 University of Zurich to Cyril Zipfel. The NMR data were acquired at CERMAX,  
670 ITQB-NOVA, Oeiras, Portugal with equipment funded by FCT. C.J.S.M. is  
671 grateful to Aralab (Portugal) for the PhD contract 06/PlantsLife/2017 and to  
672 EMBO for the short-term fellowship (#8003). RE and IM are grateful to FCT  
673 funding for the PhD scholarship BD/06435/2021 and for the working contract  
674 financed by national funds under norma transitória D.L. n.º 57/2016,  
675 respectively.

676

677 **Authors' contributions**

678 CSP and CZ supervised the project and the interpretation of data; CSP  
679 prepared the final version of the manuscript. All authors have made substantial  
680 contributions to the acquisition, analysis and interpretation of data and  
681 contributed to the drafting of the manuscript: CJSM, AB and RE (cutin and COM  
682 preparation); CJSM (all plant experiments); CJSM, MB and CM (RNA seq);  
683 AST, CJSM and RE (GC-MS); AB and RE (NMR); IM and CJSM (LC-MS/MS);  
684 BB and MF (MALDI-TOF); CJSM (preparation of the initial draft of the  
685 manuscript). All authors read and approved the final version of the manuscript.

686

687

688

689

690

## 691 **References**

- 692 **Anders S, Pyl PT, Huber W** (2015) HTSeq—a Python framework to work with high-  
693 throughput sequencing data. *Bioinformatics* **31**: 166–169
- 694 **Annarao S, Sidhu OP, Roy R, Tuli R, Khetrpal CL** (2008) Lipid profiling of developing  
695 *Jatropha curcas* L. seeds using <sup>1</sup>H NMR spectroscopy. *Bioresour Technol* **99**: 9032–  
696 9035
- 697 **de Azevedo Souza C, Li S, Lin AZ, Boutrot F, Grossmann G, Zipfel C, Somerville SC**  
698 (2017) Cellulose-derived oligomers act as damage-associated molecular patterns  
699 and trigger defense-like responses. *Plant Physiol* **173**: 2383–2398
- 700 **Beneloujaephajri E, Costa A, L’Haridon F, Métraux J-P, Binda M** (2013) Production of  
701 reactive oxygen species and wound-induced resistance in *Arabidopsis thaliana*  
702 against *Botrytis cinerea* are preceded and depend on a burst of calcium. *BMC Plant*  
703 *Biology* 2013 13:1 **13**: 1–10
- 704 **Bento A, Moreira CJS, Correia VG, Escórcio R, Rodrigues R, Tomé AS, Geneix N, Petit J,**  
705 **Bakan B, Rothan C, et al** (2021) Quantification of Structure-Property Relationships  
706 for Plant Polyesters Reveals Suberin and Cutin Idiosyncrasies. *ACS Sustain Chem*  
707 *Eng* **9**: 15780–15792
- 708 **Bhunja RK, Showman LJ, Jose A, Nikolau BJ** (2018) Combined use of cutinase and high-  
709 resolution mass-spectrometry to query the molecular architecture of cutin. *Plant*  
710 *Methods* **14**: 1–17
- 711 **Bjornson M, Pimprikar P, Nürnberger T, Zipfel C** (2021) The transcriptional landscape  
712 of *Arabidopsis thaliana* pattern-triggered immunity. *Nat Plants* **7**: 579
- 713 **Bolger AM, Lohse M, Usadel B** (2014) Trimmomatic: a flexible trimmer for Illumina  
714 sequence data. *Bioinformatics* **30**: 2114–2120
- 715 **Buxdorf K, Rubinsky G, Barda O, Burdman S, Aharoni A, Levy M** (2014) The  
716 transcription factor SISHINE3 modulates defense responses in tomato plants.  
717 *Plant Mol Biol* **84**: 37–47
- 718 **Correia VG, Bento A, Pais J, Rodrigues R, Haliński P, Frydrych M, Greenhalgh A,**  
719 **Stepnowski P, Vollrath F, King AWT, et al** (2020) The molecular structure and  
720 multifunctionality of the cryptic plant polymer suberin. *Mater Today Bio* **5**: 100039
- 721 **DeFalco TA, Zipfel C** (2021) Molecular mechanisms of early plant pattern-triggered  
722 immune signaling. *Mol Cell* **81**: 3449–3467
- 723 **Delwiche CF, Cooper ED** (2015) The evolutionary origin of a terrestrial flora. *Current*  
724 *Biology* **25**: R899–R910
- 725 **Escórcio R, Bento A, Tomé AS, Correia VG, Rodrigues R, Moreira CJS, Marion D, Bakan**  
726 **B, Silva Pereira C** (2022) Finding a Needle in a Haystack: Producing Antimicrobial  
727 Cutin-Derived Oligomers from Tomato Pomace. *ACS Sustain Chem Eng* **10**: 11415–  
728 11427

- 729 **European Commission** (2021) The tomato market in the EU: Vol. 1: Production and area  
730 statistics.
- 731 **Felix G, Duran JD, Volko S, Boller T** (1999) Plants have a sensitive perception system for  
732 the most conserved domain of bacterial flagellin. *The Plant Journal* **18**: 265–276
- 733 **Ferrari S, Savatin DV, Sicilia F, Gramegna G, Cervone F, de Lorenzo G** (2013)  
734 Oligogalacturonides: plant damage-associated molecular patterns and regulators  
735 of growth and development. *Front Plant Sci* **0**: 49
- 736 **Fich EA, Segerson NA, Rose JKC** (2016) The Plant Polyester Cutin: Biosynthesis,  
737 Structure, and Biological Roles. *Annu Rev Plant Biol* **67**: 207–233
- 738 **Hou S, Liu Z, Shen H, Wu D** (2019) Damage-Associated Molecular Pattern-Triggered  
739 Immunity in Plants. *Front Plant Sci*. doi: 10.3389/FPLS.2019.00646
- 740 **Kauss H, Fauth M, Merten A, Jeblick W** (1999) Cucumber hypocotyls respond to cutin  
741 monomers via both an inducible and a constitutive H<sub>2</sub>O<sub>2</sub>-generating system. *Plant*  
742 *Physiol* **120**: 1175–1182
- 743 **Kilian J, Whitehead D, Horak J, Wanke D, Weinl S, Batistic O, D'Angelo C, Bornberg-**  
744 **Bauer E, Kudla J, Harter K** (2007) The AtGenExpress global stress expression data  
745 set: protocols, evaluation and model data analysis of UV-B light, drought and cold  
746 stress responses. *The Plant Journal* **50**: 347–363
- 747 **Kim D, Langmead B, Salzberg SL** (2015) HISAT: a fast spliced aligner with low memory  
748 requirements. *Nature Methods* 2015 12:4 **12**: 357–360
- 749 **Kim TH, Park JH, Kim MC, Cho SH** (2008) Cutin monomer induces expression of the rice  
750 OsLTP5 lipid transfer protein gene. *J Plant Physiol* **165**: 345–349
- 751 **Kolattukudy PE, Rogers LM, Li D, Hwang CS, Flaishman MA** (1995) Surface signaling in  
752 pathogenesis. *Proc Natl Acad Sci U S A* **92**: 4080–4087
- 753 **Li W, Du W, Liu D** (2007) *Rhizopus oryzae* IFO 4697 whole cell-catalyzed methanolysis  
754 of crude and acidified rapeseed oils for biodiesel production in tert-butanol  
755 system. *Process Biochemistry* **42**: 1481–1485
- 756 **Longhi S, Cambillau C** (1999) Structure-activity of cutinase, a small lipolytic enzyme.  
757 *Biochim Biophys Acta Mol Cell Biol Lipids* **1441**: 185–196
- 758 **Love MI, Huber W, Anders S** (2014) Moderated estimation of fold change and  
759 dispersion for RNA-seq data with DESeq2. *Genome Biology* 2014 15:12 **15**: 1–21
- 760 **Macho AP, Zipfel C** (2014) Plant PRRs and the activation of innate immune signaling.  
761 *Mol Cell* **54**: 263–272
- 762 **Mao L, Luo S, Huang Q, Lu J** (2013) Horseradish Peroxidase Inactivation: Heme  
763 Destruction and Influence of Polyethylene Glycol. *Scientific Reports* 2013 3:1 **3**: 1–  
764 7
- 765 **Marc M, Risani R, Desnoes E, Falourd X, Pontoire B, Rodrigues R, Escórcio R, Batista**  
766 **AP, Valentin R, Gontard N, et al** (2021) Bioinspired co-polyesters of hydroxy-fatty  
767 acids extracted from tomato peel agro-wastes and glycerol with tunable  
768 mechanical, thermal and barrier properties. *Ind Crops Prod* **170**: 113718



- 769 **Martin LBB, Rose JKC** (2014) There's more than one way to skin a fruit: formation and  
770 functions of fruit cuticles. *J Exp Bot* **65**: 4639–4651
- 771 **Mélida H, Bacete L, Ruprecht C, Rebaque D, del Hierro I, López G, Brunner F, Pfrengle**  
772 **F, Molina A** (2020) Arabinoxylan-Oligosaccharides Act as Damage Associated  
773 Molecular Patterns in Plants Regulating Disease Resistance. *Front Plant Sci* **0**: 1210
- 774 **Mithöfer A, Mazars C** (2002) Aequorin-based measurements of intracellular Ca<sup>2+</sup>-  
775 signatures in plant cells. *Biological Procedures Online* • **4**: 105–118
- 776 **Moreira CJS, Bento A, Pais J, Petit J, Escórcio R, Correia VG, Pinheiro Â, Halinski ŁP,**  
777 **Mykhaylyk OO, Rothan C, et al** (2020) An ionic liquid extraction that preserves the  
778 molecular structure of cutin shown by nuclear magnetic resonance. *Plant Physiol.*  
779 doi: 10.1104/pp.20.01049
- 780 **Park JH, Suh MC, Kim TH, Kim MC, Cho SH** (2008) Expression of glycine-rich protein  
781 genes, AtGRP5 and AtGRP23, induced by the cutin monomer 16-hydroxypalmitic  
782 acid in *Arabidopsis thaliana*. *Plant Physiology and Biochemistry* **46**: 1015–1018
- 783 **Philippe G, Geneix N, Petit J, Guillon F, Sandt C, Rothan C, Lahaye M, Marion D, Bakan**  
784 **B** (2020a) Plant cuticle embedded polysaccharides exhibit specific structural  
785 features. *New Phytol* (in press)
- 786 **Philippe G, Geneix N, Petit J, Guillon F, Sandt C, Rothan C, Lahaye M, Marion D, Bakan**  
787 **B** (2020b) Assembly of tomato fruit cuticles: a cross-talk between the cutin  
788 polyester and cell wall polysaccharides. *New Phytologist* **226**: 809–822
- 789 **di Pietro ME, Mannu A, Mele A** (2020) NMR Determination of Free Fatty Acids in  
790 Vegetable Oils. *Processes* 2020, Vol 8, Page 410 **8**: 410
- 791 **Ranf S, Eschen-Lippold L, Pecher P, Lee J, Scheel D** (2011) Interplay between calcium  
792 signalling and early signalling elements during defence responses to microbe- or  
793 damage-associated molecular patterns. *The Plant Journal* **68**: 100–113
- 794 **Rebaque D, Hierro I del, López G, Bacete L, Vilaplana F, Dallabernardina P, Pfrengle F,**  
795 **Jordá L, Sánchez-Vallet A, Pérez R, et al** (2021) Cell wall-derived mixed-linked  $\beta$ -  
796 1,3/1,4-glucans trigger immune responses and disease resistance in plants. *The*  
797 *Plant Journal* **106**: 601–615
- 798 **Roux M, Schwessinger B, Albrecht C, Chinchilla D, Jones A, Holton N, Malinovsky FG,**  
799 **Tör M, Vries S de, Zipfel C** (2011) The *Arabidopsis* Leucine-Rich Repeat Receptor–  
800 Like Kinases BAK1/SERK3 and BKK1/SERK4 Are Required for Innate Immunity to  
801 Hemibiotrophic and Biotrophic Pathogens. *Plant Cell* **23**: 2440
- 802 **Segonzac C, Feike D, Gimenez-Ibanez S, Hann DR, Zipfel C, Rathjen JP** (2011) Hierarchy  
803 and Roles of Pathogen-Associated Molecular Pattern-Induced Responses in  
804 *Nicotiana benthamiana*. *Plant Physiol* **156**: 687
- 805 **Serrano M, Coluccia F, Torres M, L'Haridon F, Métraux J-P** (2014) The cuticle and plant  
806 defense to pathogens. *Front Plant Sci* **0**: 274
- 807 **Shi H, Bressan R** (2006) RNA Extraction. *Methods Mol Biol* **323**: 345–348

808 **Tang D, Wang G, Zhou J-M** (2017) Receptor Kinases in Plant-Pathogen Interactions:  
809 More Than Pattern Recognition. *Plant Cell* **29**: 618–637

810 **Waters ER** (2003) Molecular adaptation and the origin of land plants. *Mol Phylogenet*  
811 *Evol* **29**: 456–463

812 **Wickham H, Averick M, Bryan J, Chang W, McGowan LD, François R, Grolemond G,**  
813 **Hayes A, Henry L, Hester J, et al** (2019) Welcome to the Tidyverse. *J Open Source*  
814 *Softw* **4**: 1686

815 **Willmann R, Haischer DJ, Gust AA** (2014) Analysis of MAPK Activities Using MAPK-  
816 Specific Antibodies. *Methods in Molecular Biology* **1171**: 27–37

817 **Xin A, Fry SC** (2021) Cutin:xyloglucan transacylase (CXT) activity covalently links cutin to  
818 a plant cell-wall polysaccharide. *J Plant Physiol* **262**: 153446

819 **Xin X-F, Nomura K, Aung K, Velásquez AC, Yao J, Boutrot F, Chang JH, Zipfel C, He SY**  
820 (2016) Bacteria establish an aqueous living space in plants crucial for virulence.  
821 *Nature* **539**: 524

822 **Yeats TH, Rose JKC** (2013) The formation and function of plant cuticles. *Plant Physiol*  
823 **163**: 5–20

824 **Yu X, Feng B, He P, Shan L** (2017) From Chaos to Harmony: Responses and Signaling  
825 upon Microbial Pattern Recognition. [https://doi.org/101146/annurev-phyto-](https://doi.org/101146/annurev-phyto-080516-035649)  
826 [080516-035649](https://doi.org/101146/annurev-phyto-080516-035649) **55**: 109–137

827 **Zhu H, Jia Z, Trush MA, Li YR** (2016) A Highly Sensitive Chemiluminometric Assay for  
828 Real-Time Detection of Biological Hydrogen Peroxide Formation. *React Oxyg*  
829 *Species (Apex)* **1**: 216

830 **Zipfel C** (2014) Plant pattern-recognition receptors. *Trends Immunol* **35**: 345–351

831

832

833

834

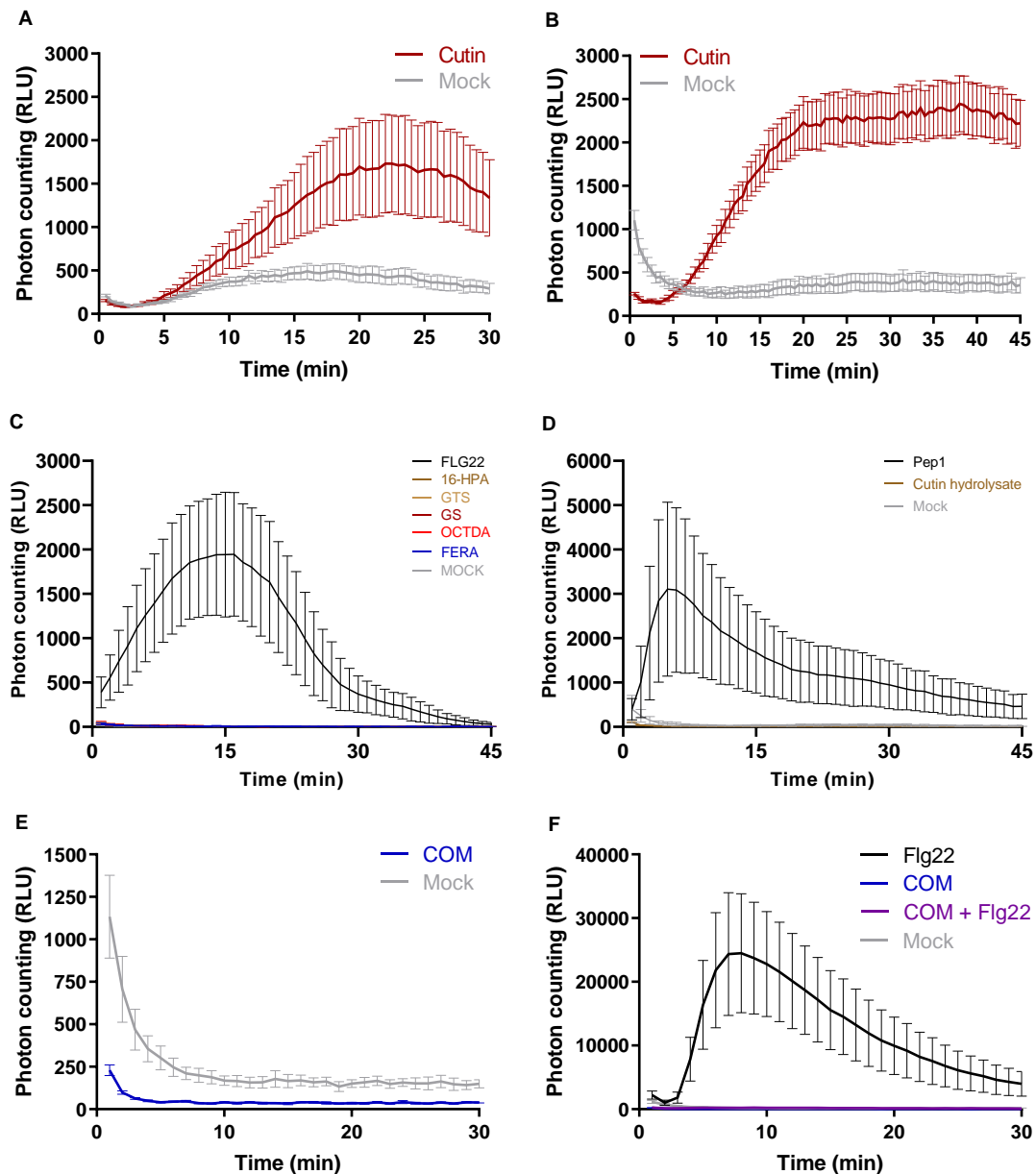


**Fig. 1** - Luminescence-based detection of apoplastic ROS in *Arabidopsis thaliana* Col-0 leaf discs upon treatment with  $2 \text{ mg}\cdot\text{mL}^{-1}$  of cutin in MiliQ water for 30 min (A) and 45 min (B); C – 1 mM of commercially available pure monomers (16-hydroxypalmitic acid (16-HPA), octanedioic acid (OCTDA) and ferulic acid (FERA)), and oligomers (glyceryl stearate (GS) and glyceryl tristearate (GTS)), in 10 % ethanol in MiliQ water for 45 min; D – 1  $\text{mg}\cdot\text{mL}^{-1}$  of cutin hydrolysate obtained after alkaline hydrolysis of cutin; E – 2  $\text{mg}\cdot\text{mL}^{-1}$  of COM obtained through the methanolysis of cutin in 0.5 % DMSO in MiliQ water; and F – co-treatment with 2  $\text{mg}\cdot\text{mL}^{-1}$  of COM and 100 nM Flg22 in 0.5 % DMSO in MiliQ water. In all the assays the Mock consists of the solvent. The positive controls were Flg22 (100 nM) or Pep1 (100 nM).

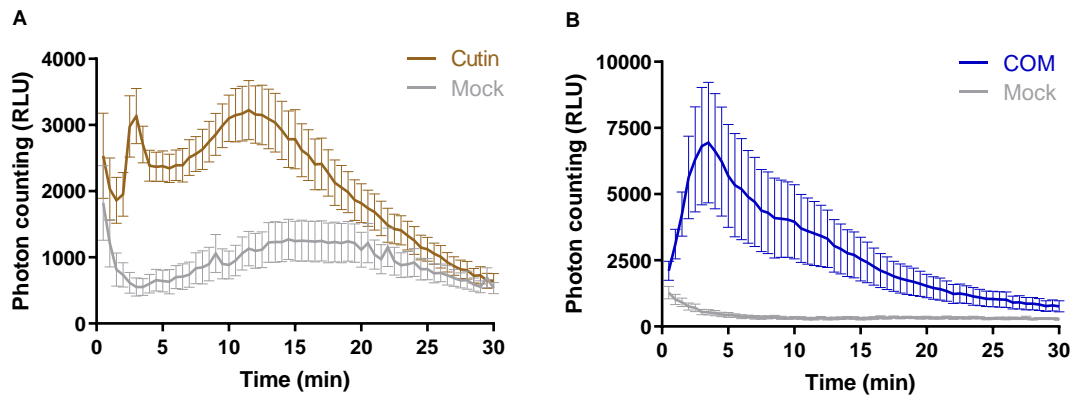


**Fig. 2** – Luminescence-based detection of calcium influx in *Arabidopsis thaliana* seedlings expressing the calcium reporter aequorin, upon treatment with: **A** – 1 mg·mL<sup>-1</sup> of cutin in MiliQ water; **B** – 2 mg·mL<sup>-1</sup> of COM in 0.5 % DMSO in MiliQ water. In all the assays the Mock consists of the solvent.

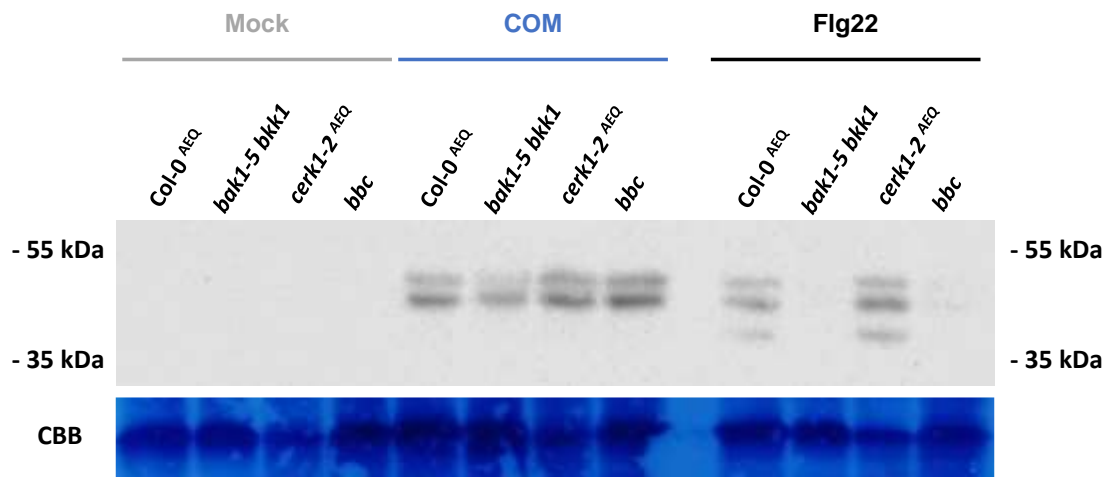


**Fig. 3** – Western blot evaluation of MAPK activation in 14-day-old *Arabidopsis thaliana* seedlings from wild type Col-0<sup>aeq</sup> plants and the *bak1-5 bkk1*, *cerk1-2<sup>aeq</sup>* and *bbc* mutants, upon treatment with 3 mg·mL<sup>-1</sup> of COM in 0.5 % DMSO in MiliQ water. The mock consists of the solvent, and the positive control was Flg22 (100 nM, in MiliQ water).

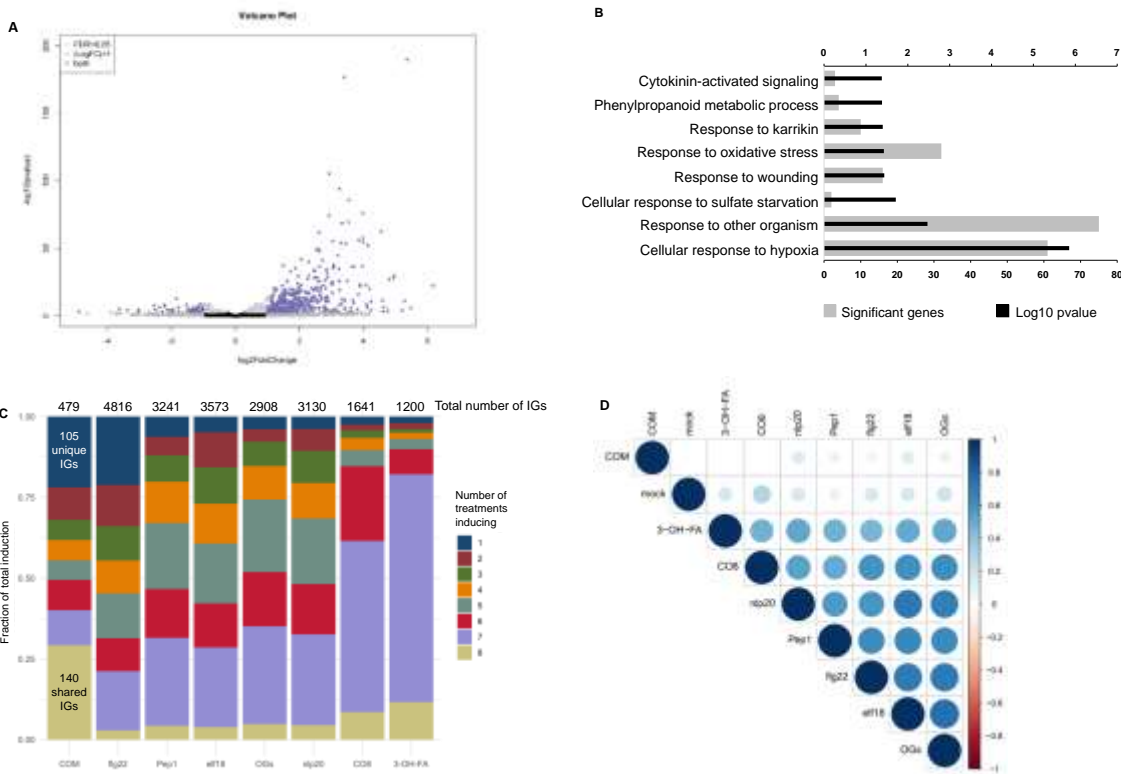
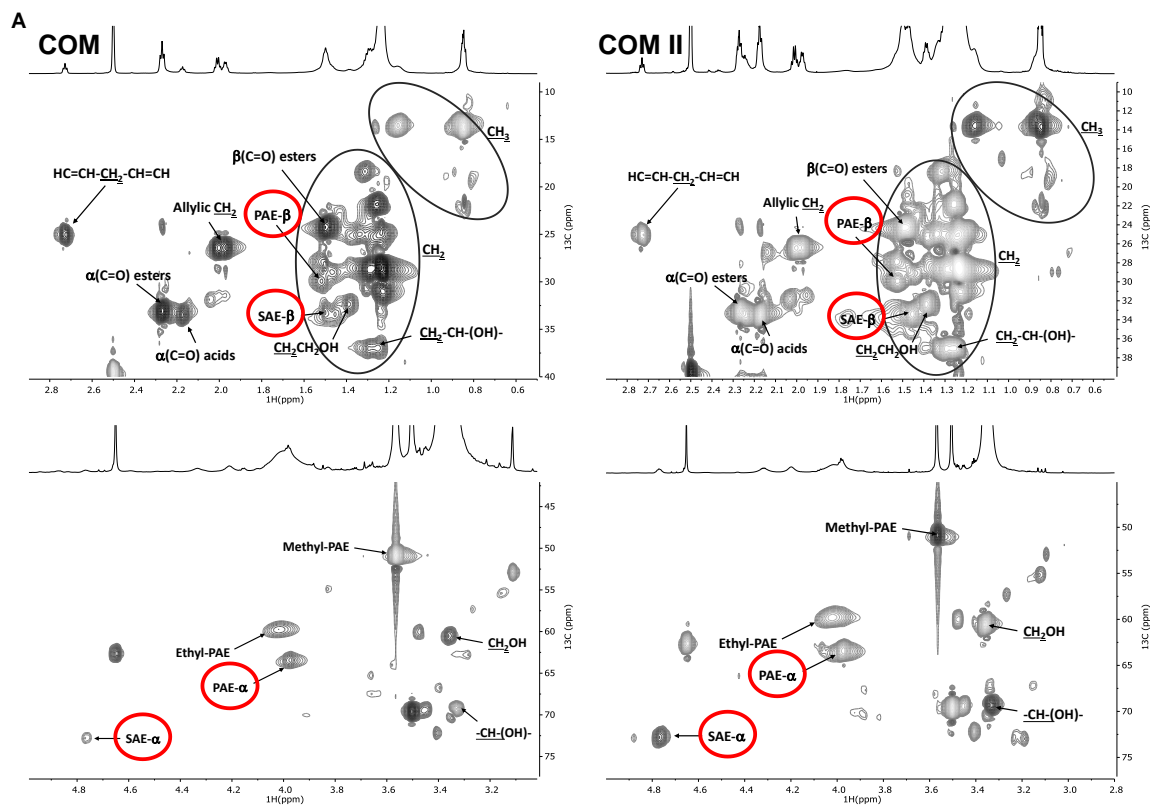


**Fig. 4 – (A)** Volcano plot representing the statistically significant (adjusted  $p$ -value  $< 0.05$ ) differentially expressed genes ( $\text{Log}_2$  fold change  $\leq -1$  or  $\geq 1$ ), in *Arabidopsis thaliana* Col-0 plants upon treatment with COM for 30 min (479 upregulated genes and 49 downregulated genes). **(B)** GO term enrichment analysis of the genes that showed upregulation upon treatment with COM for 30 min. **(C)** Comparison of genes induced by treatment of COM with those induced by seven other elicitors of plant triggered immunity. The total number of induced genes (IGs) for each elicitor (over all time points in Bjornson, *et al.* 2021) is presented and the number of genes induced by all treatments or solely by COM are highlighted. **(D)** Correlation plot depicting changes in gene expression between all the elicitors evaluated in the comparative analysis: all transcriptomes compared at 30 min post treatment.



**B**

	PAE	SAE	ME	EE	ArE	Total Esters
COM	11.16 ± 2.10	3.35 ± 0.33	68.02 ± 4.04	15.85 ± 3.03	1.62 ± 0.20	16.16 ± 2.73
COM II	24.36 ± 2.56	13.62 ± 1.51	40.79 ± 1.62	21.23 ± 1.08	<i>n.d.</i>	6.35 ± 1.83

**Fig. 5 – (A)** NMR characterization of cutin-derived COMs. Magnification of the HSQC spectral regions corresponding to aliphatics for each sample. Some correlations (unlabelled) are uncertain or unidentified. **(B)** NMR quantification of the relative abundances of esters types present in each COM calculated through the integration of signals in the corresponding  $^1\text{H}$  NMR spectra. Ester types detected on this analysis include, PAE (Primary aliphatic esters), SAE (Secondary aliphatic esters), ME (Methyl esters), EE (Ethyl esters) and ArE (Aromatic Esters). Esters that were not detected on a sample are labelled as *n.d.*

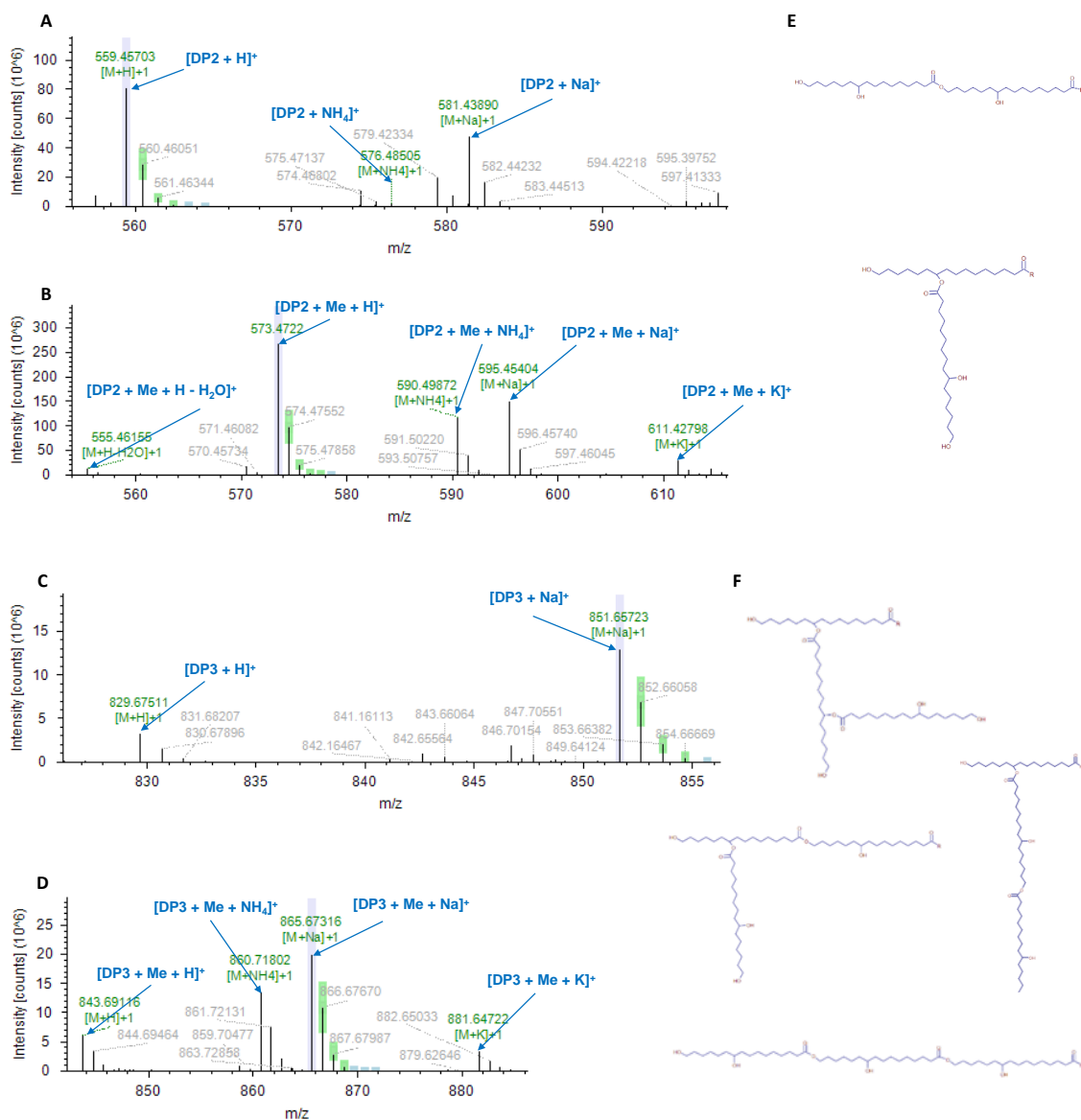


**Fig. 6** – LC-MS/MS characterization of COM II (representative spectra for both COMs) in positive mode. MS1 spectra of the detected dimer composed by ester linked molecules of 10,16-dihydroxyhexadecanoic acid (DP2) in the non-methylated (**A**) and methylated (**B**) forms. MS1 spectra of the detected trimer composed by ester linked molecules of 10,16-dihydroxyhexadecanoic acid (DP3) in the non-methylated (**C**) and methylated (**D**) forms. Possible chemical configurations of the putatively identified oligomers (**E**–**F**), where R corresponds to an OH or CH<sub>3</sub> group for the non-methylated and methylated forms, respectively. Lavender is presented when the labelled centroid matches the monoisotopic mass of the expected compound ion; Green is presented when the labelled centroid matches the delta mass and the relative intensity of the theoretic isotope pattern within the specified tolerances; Blue is presented when



the expected centroid for this  $m/z$  value might be missing because its theoretic intensity is at the level of the baseline noise. The corresponding MS2 spectra are shown in Supplemental Fig. S7.

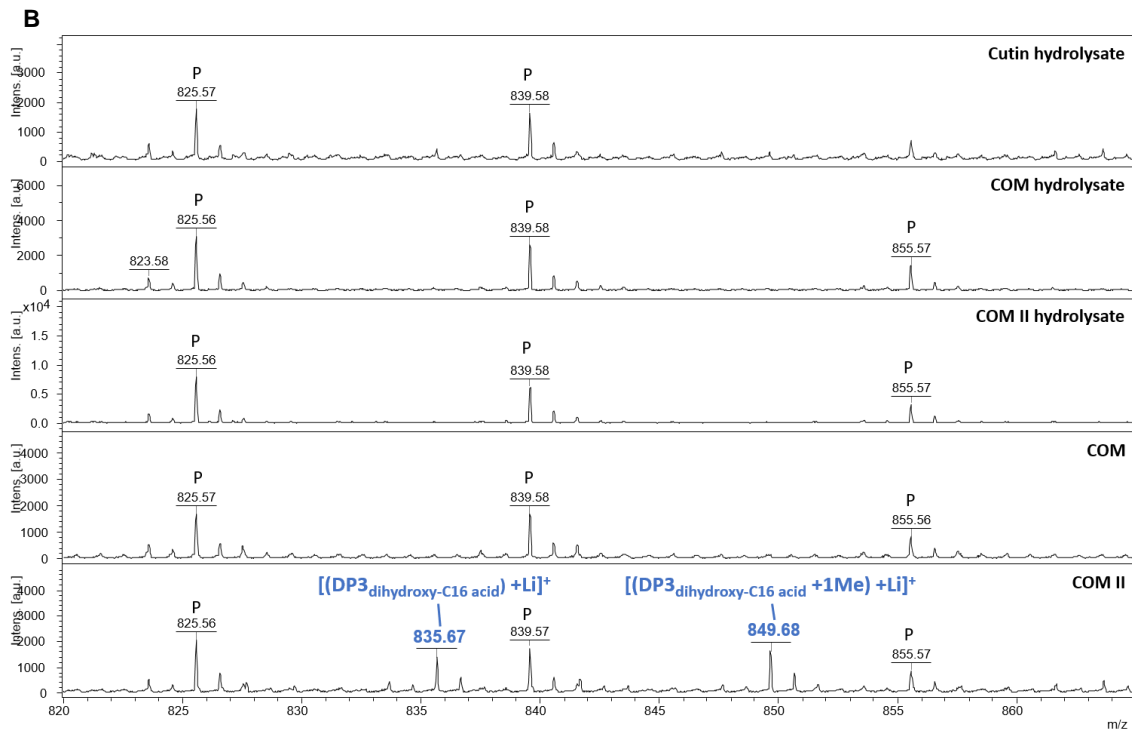
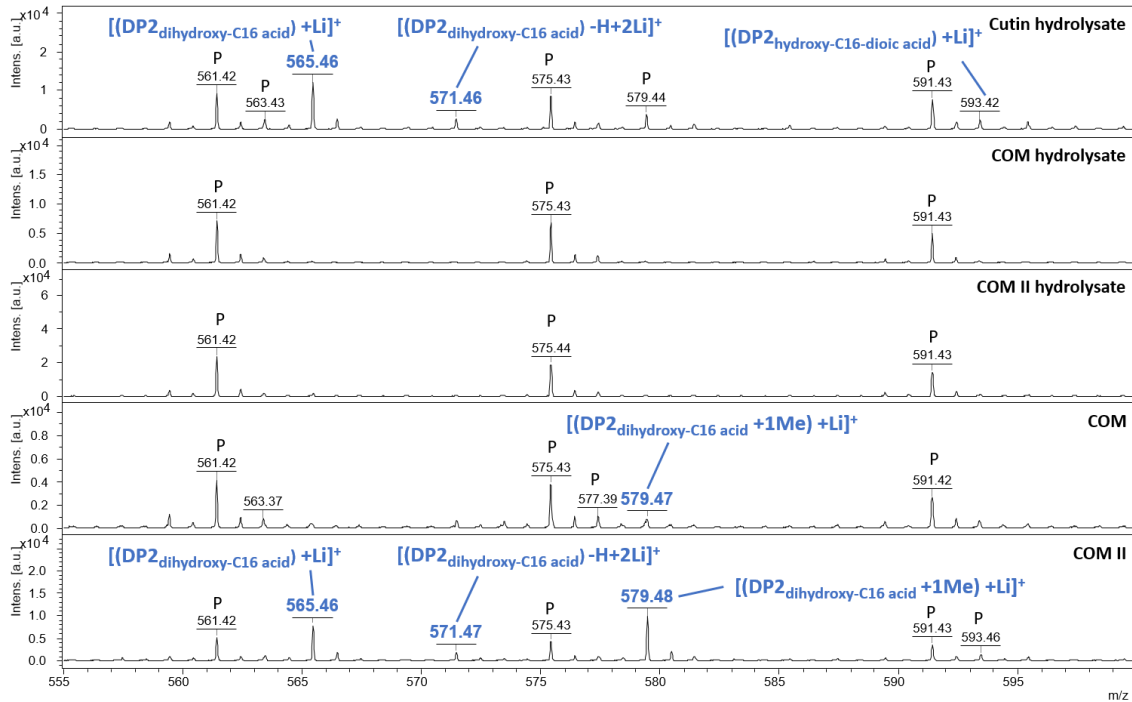


**Fig. 7** – MALDI-TOF (+) spectra of cutin hydrolysate, COMs hydrolysates and COMs. The range 555-600 Da corresponds to expected masses for DP2s (A). The range 820-865 Da corresponds to expected masses for DP3s (B). Annotations were deduced from exact mass measurements. Black star indicates an ion from the MALDI matrix. “p” indicates an ion from PEG contamination.

## Parsed Citations

Anders S, Pyl PT, Huber W (2015) HTSeq-a Python framework to work with high-throughput sequencing data. *Bioinformatics* 31: 166–169

Google Scholar: [Author Only](#) [Title Only](#) [Author and Title](#)

Annarao S, Sidhu OP, Roy R, Tuli R, Khetrapal CL (2008) Lipid profiling of developing *Jatropha curcas* L. seeds using <sup>1</sup>H NMR spectroscopy. *Bioresour Technol* 99: 9032–9035

Google Scholar: [Author Only](#) [Title Only](#) [Author and Title](#)

de Azevedo Souza C, Li S, Lin AZ, Boutrot F, Grossmann G, Zipfel C, Somerville SC (2017) Cellulose-derived oligomers act as damage-associated molecular patterns and trigger defense-like responses. *Plant Physiol* 173: 2383–2398

Google Scholar: [Author Only](#) [Title Only](#) [Author and Title](#)

Beneloujaephajri E, Costa A, L'Haridon F, Métraux J-P, Binda M (2013) Production of reactive oxygen species and wound-induced resistance in *Arabidopsis thaliana* against *Botrytis cinerea* preceded and depend on a burst of calcium. *BMC Plant Biology* 2013 13:1 13: 1–10

Google Scholar: [Author Only](#) [Title Only](#) [Author and Title](#)

Bento A, Moreira CJS, Correia VG, Escórcio R, Rodrigues R, Tomé AS, Geneix N, Petit J, Bakan B, Rothan C, et al (2021) Quantification of Structure-Property Relationships for Plant Polyesters Reveals Suberin and Cutin Idiosyncrasies. *ACS Sustain Chem Eng* 9: 15780–15792

Google Scholar: [Author Only](#) [Title Only](#) [Author and Title](#)

Bhunja RK, Showman LJ, Jose A, Nikolau BJ (2018) Combined use of cutinase and high-resolution mass-spectrometry to query the molecular architecture of cutin. *Plant Methods* 14: 1–17

Google Scholar: [Author Only](#) [Title Only](#) [Author and Title](#)

Bjornson M, Pimprikar P, Nürnberger T, Zipfel C (2021) The transcriptional landscape of *Arabidopsis thaliana* pattern-triggered immunity. *Nat Plants* 7: 579

Google Scholar: [Author Only](#) [Title Only](#) [Author and Title](#)

Bolger AM, Lohse M, Usadel B (2014) Trimmomatic: a flexible trimmer for Illumina sequence data. *Bioinformatics* 30: 2114–2120

Google Scholar: [Author Only](#) [Title Only](#) [Author and Title](#)

Buxdorf K, Rubinsky G, Barda O, Burdman S, Aharoni A, Levy M (2014) The transcription factor SISHINE3 modulates defense responses in tomato plants. *Plant Mol Biol* 84: 37–47

Google Scholar: [Author Only](#) [Title Only](#) [Author and Title](#)

Correia VG, Bento A, Pais J, Rodrigues R, Haliński P, Frydrych M, Greenhalgh A, Stepnowski P, Vollrath F, King AWT, et al (2020) The molecular structure and multifunctionality of the cryptic plant polymer suberin. *Mater Today Bio* 5: 100039

Google Scholar: [Author Only](#) [Title Only](#) [Author and Title](#)

DeFalco TA, Zipfel C (2021) Molecular mechanisms of early plant pattern-triggered immune signaling. *Mol Cell* 81: 3449–3467

Google Scholar: [Author Only](#) [Title Only](#) [Author and Title](#)

Delwiche CF, Cooper ED (2015) The evolutionary origin of a terrestrial flora. *Current Biology* 25: R899–R910

Google Scholar: [Author Only](#) [Title Only](#) [Author and Title](#)

Escórcio R, Bento A, Tomé AS, Correia VG, Rodrigues R, Moreira CJS, Marion D, Bakan B, Silva Pereira C (2022) Finding a Needle in a Haystack: Producing Antimicrobial Cutin-Derived Oligomers from Tomato Pomace. *ACS Sustain Chem Eng* 10: 11415–11427

Google Scholar: [Author Only](#) [Title Only](#) [Author and Title](#)

European Commission (2021) The tomato market in the EU: Vol. 1: Production and area statistics.

Google Scholar: [Author Only](#) [Title Only](#) [Author and Title](#)

Felix G, Duran JD, Volko S, Boller T (1999) Plants have a sensitive perception system for the most conserved domain of bacterial flagellin. *The Plant Journal* 18: 265–276

Google Scholar: [Author Only](#) [Title Only](#) [Author and Title](#)

Ferrari S, Savatin DV, Sicilia F, Gramegna G, Cervone F, de Lorenzo G (2013) Oligogalacturonides: plant damage-associated molecular patterns and regulators of growth and development. *Front Plant Sci* 0: 49

Google Scholar: [Author Only](#) [Title Only](#) [Author and Title](#)

Fich EA, Segerson NA, Rose JKC (2016) The Plant Polyester Cutin: Biosynthesis, Structure, and Biological Roles. *Annu Rev Plant Biol* 67: 207–233

Google Scholar: [Author Only](#) [Title Only](#) [Author and Title](#)

Hou S, Liu Z, Shen H, Wu D (2019) Damage-Associated Molecular Pattern-Triggered Immunity in Plants. *Front Plant Sci*. doi:

10.3389/FPLS.2019.00646

Google Scholar: [Author Only](#) [Title Only](#) [Author and Title](#)

**Kauss H, Fauth M, Merten A, Jeblick W (1999) Cucumber hypocotyls respond to cutin monomers via both an inducible and a constitutive H<sub>2</sub>O<sub>2</sub>-generating system. *Plant Physiol* 120: 1175–1182**

Google Scholar: [Author Only](#) [Title Only](#) [Author and Title](#)

**Kilian J, Whitehead D, Horak J, Wanke D, Weini S, Batistic O, D'Angelo C, Bornberg-Bauer E, Kudla J, Harter K (2007) The *AtGenExpress* global stress expression data set: protocols, evaluation and model data analysis of UV-B light, drought and cold stress responses. *The Plant Journal* 50: 347–363**

Google Scholar: [Author Only](#) [Title Only](#) [Author and Title](#)

**Kim D, Langmead B, Salzberg SL (2015) HISAT: a fast spliced aligner with low memory requirements. *Nature Methods* 2015 12:4 12: 357–360**

Google Scholar: [Author Only](#) [Title Only](#) [Author and Title](#)

**Kim TH, Park JH, Kim MC, Cho SH (2008) Cutin monomer induces expression of the rice OsLTP5 lipid transfer protein gene. *J Plant Physiol* 165: 345–349**

Google Scholar: [Author Only](#) [Title Only](#) [Author and Title](#)

**Kolattukudy PE, Rogers LM, Li D, Hwang CS, Flaishman MA (1995) Surface signaling in pathogenesis. *Proc Natl Acad Sci U S A* 92: 4080–4087**

Google Scholar: [Author Only](#) [Title Only](#) [Author and Title](#)

**Li W, Du W, Liu D (2007) *Rhizopus oryzae* IFO 4697 whole cell-catalyzed methanolysis of crude and acidified rapeseed oils for biodiesel production in tert-butanol system. *Process Biochemistry* 42: 1481–1485**

Google Scholar: [Author Only](#) [Title Only](#) [Author and Title](#)

**Longhi S, Cambillau C (1999) Structure-activity of cutinase, a small lipolytic enzyme. *Biochim Biophys Acta Mol Cell Biol Lipids* 1441: 185–196**

Google Scholar: [Author Only](#) [Title Only](#) [Author and Title](#)

**Love MI, Huber W, Anders S (2014) Moderated estimation of fold change and dispersion for RNA-seq data with DESeq2. *Genome Biology* 2014 15:12 15: 1–21**

Google Scholar: [Author Only](#) [Title Only](#) [Author and Title](#)

**Macho AP, Zipfel C (2014) Plant PRRs and the activation of innate immune signaling. *Mol Cell* 54: 263–272**

Google Scholar: [Author Only](#) [Title Only](#) [Author and Title](#)

**Mao L, Luo S, Huang Q, Lu J (2013) Horseradish Peroxidase Inactivation: Heme Destruction and Influence of Polyethylene Glycol. *Scientific Reports* 2013 3:1 3: 1–7**

Google Scholar: [Author Only](#) [Title Only](#) [Author and Title](#)

**Marc M, Risani R, Desnoes E, Falourd X, Pontoire B, Rodrigues R, Escórcio R, Batista AP, Valentin R, Gontard N, et al (2021) Bioinspired co-polyesters of hydroxy-fatty acids extracted from tomato peel agro-wastes and glycerol with tunable mechanical, thermal and barrier properties. *Ind Crops Prod* 170: 113718**

Google Scholar: [Author Only](#) [Title Only](#) [Author and Title](#)

**Martin LBB, Rose JKC (2014) There's more than one way to skin a fruit: formation and functions of fruit cuticles. *J Exp Bot* 65: 4639–4651**

Google Scholar: [Author Only](#) [Title Only](#) [Author and Title](#)

**Mélida H, Bacete L, Ruprecht C, Rebaque D, del Hierro I, López G, Brunner F, Pfrengle F, Molina A (2020) Arabinoxylan-Oligosaccharides Act as Damage Associated Molecular Patterns in Plants Regulating Disease Resistance. *Front Plant Sci* 0: 1210**

Google Scholar: [Author Only](#) [Title Only](#) [Author and Title](#)

**Mithöfer A, Mazars C (2002) Aequorin-based measurements of intracellular Ca<sup>2+</sup>-signatures in plant cells. *Biological Procedures Online* • 4: 105–118**

Google Scholar: [Author Only](#) [Title Only](#) [Author and Title](#)

**Moreira CJS, Bento A, Pais J, Petit J, Escórcio R, Correia VG, Pinheiro Â, Halinski ŁP, Mykhaylyk OO, Rothan C, et al (2020) An ionic liquid extraction that preserves the molecular structure of cutin shown by nuclear magnetic resonance. *Plant Physiol*. doi: 10.1104/pp.20.01049**

Google Scholar: [Author Only](#) [Title Only](#) [Author and Title](#)

**Park JH, Suh MC, Kim TH, Kim MC, Cho SH (2008) Expression of glycine-rich protein genes, *AtGRP5* and *AtGRP23*, induced by the cutin monomer 16-hydroxypalmitic acid in *Arabidopsis thaliana*. *Plant Physiology and Biochemistry* 46: 1015–1018**

Google Scholar: [Author Only](#) [Title Only](#) [Author and Title](#)

**Philippe G, Geneix N, Petit J, Guillon F, Sandt C, Rothan C, Lahaye M, Marion D, Bakan B (2020a) Plant cuticle embedded**

**polysaccharides exhibit specific structural features. *New Phytol* (in press)**

Google Scholar: [Author Only](#) [Title Only](#) [Author and Title](#)

**Philippe G, Geneix N, Petit J, Guillon F, Sandt C, Rothan C, Lahaye M, Marion D, Bakan B (2020b) Assembly of tomato fruit cuticles: a cross-talk between the cutin polyester and cell wall polysaccharides. *New Phytologist* 226: 809–822**

Google Scholar: [Author Only](#) [Title Only](#) [Author and Title](#)

**di Pietro ME, Mannu A, Mele A (2020) NMR Determination of Free Fatty Acids in Vegetable Oils. *Processes* 2020, Vol 8, Page 410 8: 410**

Google Scholar: [Author Only](#) [Title Only](#) [Author and Title](#)

**Ranf S, Eschen-Lippold L, Pecher P, Lee J, Scheel D (2011) Interplay between calcium signalling and early signalling elements during defence responses to microbe- or damage-associated molecular patterns. *The Plant Journal* 68: 100–113**

Google Scholar: [Author Only](#) [Title Only](#) [Author and Title](#)

**Rebaque D, Hierro I del, López G, Bacete L, Vilaplana F, Dallabernardina P, Pfrengle F, Jordá L, Sánchez-Vallet A, Pérez R, et al (2021) Cell wall-derived mixed-linked  $\beta$ -1,3/1,4-glucans trigger immune responses and disease resistance in plants. *The Plant Journal* 106: 601–615**

Google Scholar: [Author Only](#) [Title Only](#) [Author and Title](#)

**Roux M, Schwessinger B, Albrecht C, Chinchilla D, Jones A, Holton N, Malinovskiy FG, Tör M, Vries S de, Zipfel C (2011) The Arabidopsis Leucine-Rich Repeat Receptor–Like Kinases BAK1/SERK3 and BKK1/SERK4 Are Required for Innate Immunity to Hemibiotrophic and Biotrophic Pathogens. *Plant Cell* 23: 2440**

Google Scholar: [Author Only](#) [Title Only](#) [Author and Title](#)

**Segonzac C, Feike D, Gimenez-Ibanez S, Hann DR, Zipfel C, Rathjen JP (2011) Hierarchy and Roles of Pathogen-Associated Molecular Pattern-Induced Responses in *Nicotiana benthamiana*. *Plant Physiol* 156: 687**

Google Scholar: [Author Only](#) [Title Only](#) [Author and Title](#)

**Serrano M, Coluccia F, Torres M, L'Haridon F, Métraux J-P (2014) The cuticle and plant defense to pathogens. *Front Plant Sci* 0: 274**

Google Scholar: [Author Only](#) [Title Only](#) [Author and Title](#)

**Shi H, Bressan R (2006) RNA Extraction. *Methods Mol Biol* 323: 345–348**

Google Scholar: [Author Only](#) [Title Only](#) [Author and Title](#)

**Tang D, Wang G, Zhou J-M (2017) Receptor Kinases in Plant-Pathogen Interactions: More Than Pattern Recognition. *Plant Cell* 29: 618–637**

Google Scholar: [Author Only](#) [Title Only](#) [Author and Title](#)

**Waters ER (2003) Molecular adaptation and the origin of land plants. *Mol Phylogenet Evol* 29: 456–463**

Google Scholar: [Author Only](#) [Title Only](#) [Author and Title](#)

**Wickham H, Averick M, Bryan J, Chang W, McGowan LD, François R, Grolemond G, Hayes A, Henry L, Hester J, et al (2019) Welcome to the Tidyverse. *J Open Source Softw* 4: 1686**

Google Scholar: [Author Only](#) [Title Only](#) [Author and Title](#)

**Willmann R, Haischer DJ, Gust AA (2014) Analysis of MAPK Activities Using MAPK-Specific Antibodies. *Methods in Molecular Biology* 1171: 27–37**

Google Scholar: [Author Only](#) [Title Only](#) [Author and Title](#)

**Xin A, Fry SC (2021) Cutin:xyloglucan transacylase (CXT) activity covalently links cutin to a plant cell-wall polysaccharide. *J Plant Physiol* 262: 153446**

Google Scholar: [Author Only](#) [Title Only](#) [Author and Title](#)

**Xin X-F, Nomura K, Aung K, Velásquez AC, Yao J, Boutrot F, Chang JH, Zipfel C, He SY (2016) Bacteria establish an aqueous living space in plants crucial for virulence. *Nature* 539: 524**

Google Scholar: [Author Only](#) [Title Only](#) [Author and Title](#)

**Yeats TH, Rose JKC (2013) The formation and function of plant cuticles. *Plant Physiol* 163: 5–20**

Google Scholar: [Author Only](#) [Title Only](#) [Author and Title](#)

**Yu X, Feng B, He P, Shan L (2017) From Chaos to Harmony: Responses and Signaling upon Microbial Pattern Recognition. <https://doi.org/10.1146/annurev-phyto-080516-035649> 55: 109–137**

Google Scholar: [Author Only](#) [Title Only](#) [Author and Title](#)

**Zhu H, Jia Z, Trush MA, Li YR (2016) A Highly Sensitive Chemiluminometric Assay for Real-Time Detection of Biological Hydrogen Peroxide Formation. *React Oxyg Species (Apex)* 1: 216**

Google Scholar: [Author Only](#) [Title Only](#) [Author and Title](#)

**Zipfel C (2014) Plant pattern-recognition receptors. *Trends Immunol* 35: 345–351**

